Uchiyama Y: The expression of tripeptidyl peptidase I in various tissues of rats and mice. Arch Histol Cytol 2002, 65:219–232
33. Fujimoto K: Freeze-fracture replica electron microscopy combined with SDS digestion for cytochemical labeling of integral membrane proteins. Application to the immunogold labeling of intercellular junctional complexes. J Cell Sci 1995, 108:3443–3449
34. Towbin H, Staehelin T, Gordon J: Electrophoretic transfer of proteins from polyacrylamide gels to nitrocellulose sheets: procedure and some applications. Proc Natl Acad Sci USA 1979, 76:4350–4354
35. Ohsawa Y, Zhang G, Kametaka S, Shibata M, Koike M, Waguri S, Uchiyama Y: Purification, cDNA cloning, and secretory properties of FLRG protein from PC12 cells and the distribution of FLRG mRNA and protein in rat tissues. Arch Histol Cytol 2003, 66:367–381
36. Dunn Jr WA: Autophagy and related mechanisms of lysosome-mediated protein degradation. Trends Cell Biol 1994, 4:139–143
37. Mann SS, Hammarback JA: Gene localization and developmental expression of light chain 3: a common subunit of microtubule-associated protein 1A(MAP1A) and MAP1B. J Neurosci Res 1996, 43:535–544
38. Roizin L, Stellar S, Willson N, Whittier J, Liu JC: Electron microscope and enzyme studies in cerebral biopsies of Huntington's chorea. Trans Am Neurol Assoc 1974, 99:240–243
39. Tellez-Nagel I, Johnson AB, Terry RD: Studies on brain biopsies of patients with Huntington's chorea. J Neuropathol Exp Neurol 1974, 33:308–332
40. Kegel KB, Kim M, Sapp E, McIntyre C, Castano JG, Aronin N, DiFiglia M: Huntington expression stimulates endosomal-lysosomal activity, endosome tubulation, and autophagy. J Neurosci 2000, 20: 7268–7278
41. Cataldo AM, Hamilton DJ, Barnett JL, Paskevich PA, Nixon RA: Properties of the endosomal-lysosomal system in the human central nervous system: disturbances mark most neurons in populations at risk to degenerate in Alzheimer's disease. J Neurosci 1996, 16:186–199
42. Stadelmann C, Deckwerth TL, Srinivasan A, Bancher C, Bruck W, Jellinger K, Lassmann H: Activation of caspase-3 in single neurons and autophagic granules of granulovacuolar degeneration in Alzheimer's disease. Evidence for apoptotic cell death. Am J Pathol 1999, 155:1459–1466
43. Yu WH, Kumar A, Peterhoff C, Shapiro Kulnane L, Uchiyama Y, Lamb BT, Cuervo AM, Nixon RA: Autophagic vacuoles are enriched in amyloid precursor protein-secretase activities: implications for beta-amyloid peptide over-production and localization in Alzheimer's disease. Int J Biochem Cell Biol 2004, 36:2531–2540
44. Anglade P, Vyas S, Javoy-Agid F, Herrero MT, Michel PP, Marquez J, Mouatt-Prigent A, Ruberg M, Hirsch EC, Agid Y: Apoptosis and autophagy in nigral neurons of patients with Parkinson's disease. Histol Histopathol 1997, 12:25–31
45. Boellaard JW, Schlote W, Tateishi J: Neuronal autophagy in experimental Creutzfeldt-Jakob's disease. Acta Neuropathol (Berl) 1989, 78:410–418
46. Boellaard JW, Kao M, Schlote W, Diringer H: Neuronal autophagy in experimental scrapie. Acta Neuropathol (Berl) 1991, 82:225–228
47. Jeffrey M, Scott JR, Williams A, Fraser H: Ultrastructural features of spongiform encephalopathy transmitted to mice from three species of bovidae. Acta Neuropathol (Berl) 1992, 84:559–569
48. Baudhuin P, Hers HG, Loeb H: An electron microscopic and biochemical study of type II glycogenosis. Lab Invest 1964, 13:1139–1152
49. Novikoff AB: Lysosomes in nerve cells. The Neuron. Edited by Hyden H. Amsterdam, Elsevier Publishing Company, 1967, pp 319–377
50. Ivy GO: Protease inhibitors as a model for NCL disease, with special emphasis on the infantile and adult forms. Am J Med Genet 1992, 42:555–560
51. Suzuki T, Nakagawa M, Yoshikawa A, Sasagawa N, Yoshimori T, Ohsumi Y, Nishino I, Ishiura S, Nonaka I: The first molecular evidence that autophagy relates rimmed vacuole formation in chloroquine myopathy. J Biochem (Tokyo) 2002, 131:647–651
52. Komatsu M, Waguri S, Ueno T, Iwata J, Murata S, Tanida I, Ezaki J, Mizushima N, Ohsumi Y, Uchiyama Y, Kominami E, Tanaka K, Chiba T: Impairment of starvation-induced and constitutive autophagy in Atg7-deficient mice. J Cell Biol 2005, 169:425–434
53. Zhan SS, Beyreuther K, Schmitt HP: Neuronal ubiquitin and neurofilament expression in different lysosomal storage disorders. Clin Neuropathol 1992, 11:251–255
54. Ardley HC, Hung CC, Robinson PA: The aggravating role of the ubiquitin-proteasome system in neurodegeneration. FEBS Lett 2005, 579:571–576
55. Tanida I, Minematsu-Ikeguchi N, Ueno T, Kominami E: Lysosomal turnover, but not a cellular level, of endogenous LC3 is a marker for autophagy. Autophagy 2005, 1:84–91
56. Asanuma K, Tanida I, Shirato I, Ueno T, Takahara H, Nishitani T, Kominami E, Tomino Y: MAP-LC3, a promising autophagosomal marker, is processed during the differentiation and recovery of podocytes from PAN nephrosis. FASEB J 2003, 17:1165–1167
57. Hollenbeck PJ: Products of endocytosis and autophagy are retrieved from axons by regulated retrograde organelle transport. J Cell Biol 1993, 121:305–315
58. Larsen KE, Fon EA, Hastings TG, Edwards RH, Sulzer D: Methamphetamine-induced degeneration of dopaminergic neurons involves autophagy and upregulation of dopamine synthesis. J Neurosci 2002, 22:8951–8960
59. Lin WL, Lewis J, Yen SH, Hutton M, Dickson DW: Ultrastructural neuronal pathology in transgenic mice expressing mutant (P301L) human tau. J Neurocytol 2003, 32:1091–1105
60. Bednarski E, Ribak CE, Lynch G: Suppression of cathepsins B and L causes a proliferation of lysosomes and the formation of meganeurites in hippocampus. J Neurosci 1997, 17:4006–4021
61. Nixon RA, Wegiel J, Kumar A, Yu WH, Peterhoff C, Cataldo A, Cuervo AM: Extensive involvement of autophagy in Alzheimer disease: an immuno-electron microscopy study. J Neuropathol Exp Neurol 2005, 64:113–122
62. Mizushima N, Yamamoto A, Hatano M, Kobayashi Y, Kabeya Y, Suzuki K, Tokuhisa T, Ohsumi Y, Yoshimori T: Dissection of autophagosome formation using Apg5-deficient mouse embryonic stem cells. J Cell Biol 2001, 152:657–668
63. Eskelinen EL, Schmidt CK, Neu S, Willenborg M, Fuertes G, Salvador N, Tanaka Y, Lullmann-Rauch R, Hartmann D, Heeren J, von Figura K, Knecht E, Saftig P: Disturbed cholesterol traffic but normal proteolytic function in LAMP-1/LAMP-2 double-deficient fibroblasts. Mol Biol Cell 2004, 15:3132–3145

Journal of Neuroscience Research 81:776–788 (2005)

Enhanced Proliferation of Progenitor Cells in the Subventricular Zone and Limited Neuronal Production in the Striatum and Neocortex of Adult Macaque Monkeys After Global Cerebral Ischemia

Anton B. Tonchev,[1,2] Tetsumori Yamashima,[1]* Kazunobu Sawamoto,[3,4] and Hideyuki Okano[4]

[1]Department of Restorative Neurosurgery, Division of Neuroscience, Kanazawa University Graduate School of Medical Sciences, Kanazawa, Japan
[2]Division of Cell Biology, Department of Forensic Medicine, Varna University of Medicine, Varna, Bulgaria
[3]Bridgestone Laboratory of Developmental and Regenerative Neurobiology, Keio University School of Medicine, Tokyo, Japan
[4]Department of Physiology, Keio University School of Medicine, Tokyo, Japan

Cerebral ischemia in adult rodent models increases the proliferation of endogenous neural progenitor cells residing in the subventricular zone along the anterior horn of the lateral ventricle (SVZa) and induces neurogenesis in the postischemic striatum and cortex. Whether the adult primate brain preserves a similar ability in response to an ischemic insult is uncertain. We used the DNA synthesis indicator bromodeoxyuridine (BrdU) to label newly generated cells in adult macaque monkeys and show here that the proliferation of cells with a progenitor phenotype (double positive for BrdU and the markers Musashi1, Nestin, and βIII-tubulin) in SVZa increased during the second week after a 20-min transient global brain ischemia. Subsequent progenitor migration seemed restricted to the rostral migratory stream toward the olfactory bulb and ischemia increased the proportion of adult-generated cells retaining their location in SVZa with a progenitor phenotype. Despite the lack of evidence for progenitor cell migration toward the postischemic striatum or prefrontal neocortex, a small but sustained proportion of BrdU-labeled cells expressed features of postmitotic neurons (positive for the protein NeuN and the transcription factors Tbr1 and Islet1) in these two regions for at least 79 days after ischemia. Taken together, our data suggest an enhanced neurogenic response in the adult primate telencephalon after a cerebral ischemic insult.

Key words: monkey; cerebral ischemia; progenitor cell; neurogenesis; gliogenesis

The adult mammalian brain retains a limited ability for neuronal regeneration by progenitor cells residing in two well-recognized neurogenic niches: the subventricular zone (SVZ) of the lateral ventricle and the subgranular zone (SGZ) of the hippocampal dentate gyrus (DG; Gage, 2000). Extensively studied in rodents, in vivo neurogenesis has also been demonstrated in SVZ (Kornack and Rakic, 2001a; Pencea et al., 2001) and SGZ (Eriksson et al., 1998; Gould et al., 1999a; Kornack and Rakic, 1999) of healthy primates, but its existence outside these regions under normal conditions remains controversial (Gould et al., 1999b, 2001; Kornack and Rakic, 2001b; Bedard et al., 2002; Koketsu et al., 2003).

In the rodent brain, cerebral ischemia increases proliferation and neuronal differentiation of neural progenitor cells in both global (Liu et al., 1998; Kee et al., 2001; Yagita et al., 2001; Nakatomi et al., 2002; Iwai et al., 2003) and focal (Jin et al., 2001; Zhang et al., 2001; Arvidsson et al., 2002; Parent et al., 2002) ischemic models. The newly generated cells have been reported to replace neurons in the postischemic hippocampus (Liu et al., 1998; Kee et al., 2001; Yagita et al.,

Supplementary Material for this article is available online at http://www.mrw.interscience.wiley.com/suppmat/0360-4012/suppmat/(www.interscience.wiley.com).

Contract grant sponsor: Japanese Ministry of Education, Culture, Sports, Science and Technology; Contract grant sponsor: National Science Fund of Bulgaria; Contract grant number: L1311/03.

*Correspondence to: Dr. Tetsumori Yamashima, Department of Restorative Neurosurgery, Division of Neuroscience, Kanazawa University Graduate School of Medical Sciences, Takara-machi 13-1, 920-8641 Kanazawa, Japan. E-mail: yamashim@med.kanazawa-u.ac.jp

Received 27 March 2005; Revised 14 May 2005; Accepted 27 May 2005

Published online 26 July 2005 in Wiley InterScience (www.interscience.wiley.com). DOI: 10.1002/jnr.20604

2001; Nakatomi et al., 2002), striatum (Arvidsson et al., 2002; Parent et al., 2002; Zhang et al., 2004), olfactory bulb (Iwai et al., 2003), and cortex (Gu et al., 2000; Nakatomi et al., 2002). Interestingly, progenitor cells in the rostral migratory stream, originally destined to become olfactory bulb neurons, are redirected toward the injured striatum and cortex after ischemia (Jin et al., 2003). In our previous study we investigated the subventricular zone along the inferior horn of the lateral ventricle (SVZi) and DG of adult monkeys after ischemia (Tonchev et al., 2003a). We found that although an increase in postischemic precursor cells was observed in the monkey DG (similar to the situation in rodents), the monkey response was much smaller than was the rodent response (Liu et al., 1998; Kee et al., 2001), in terms of the proliferation and extent of the neuronal differentiation of progenitor cells.

In this study, we used the same monkey model but focused on different brain regions. Our first goal was to monitor the phenotype and behavior of newly generated cells in SVZ of the anterior horn of the lateral ventricle (SVZa) after 20 min of global brain ischemia in adult monkeys. The adult-born cells were labeled with the thymidine analogue bromodeoxyuridine (BrdU) and the immunophenotype of BrdU-positive (BrdU+) cells was determined using a panel of selective cell markers at various times after the insult. Our second goal was to explore the potential route(s) of SVZa progenitor cell migration after ischemia. Our third goal was to identify the immunophenotype of BrdU+ cells in the postischemic striatum and neocortex. Ischemia caused an equal for the two hemispheres neuronal damage of 30–40% in these regions, using the same ischemic model used in the present study (Yoshida et al., 2002). This injury was much less pronounced than was the damage inflicted to the hippocampal CA1 sector, which exhibited an almost complete neuronal loss (Yamashima et al., 1998; Yamashima, 2000). It was also much less pronounced than the striatal/cortical injuries induced by experimental focal ischemic infarction (Arvidsson et al., 2002; Parent et al., 2002). We thus investigated progenitor cell proliferation and phenotype in the context of a moderate ischemic injury.

MATERIALS AND METHODS

Surgical Procedures

All experimental procedures were carried out in strict adherence to the guidelines of the Animal Care and Ethics Committee of Kanazawa University and the NIH Guide for the Care and Use of Laboratory Animals. The monkeys (female *Macaca fuscata*) were bred in air-conditioned cages and were allowed free daily access to food and water. Under sterile conditions and a general anesthesia with artificial ventilation, 19 adult (5–11 years old) macaques underwent transient, complete, whole brain ischemia ($n = 12$) or a sham surgery ($n = 7$), as described previously (Yamashima et al., 1998; Yamashima, 2000; Tonchev et al., 2003a). Briefly, the chest was opened, the sternum was removed, and the innominate and left subclavian arteries were transiently clipped for 20 min. The effectiveness of clipping was demonstrated by an almost complete absence (0.5 ± 1.0 ml/100 g brain/min) of cerebral blood flow, as monitored using a laser Doppler (Vasamedics, St. Paul, MN). One neonatal monkey was sacrificed on postnatal day 14 (P14), without any preceding surgery.

BrdU Labeling

All 19 adult monkeys received daily injections (100 mg/kg, intravenously) of BrdU (Sigma) for 5 consecutive days. The animals in the short-term survival group ($n = 9$) were sacrificed 2 hr after the last injection on days 4 ($n = 2$), 9 ($n = 2$) and 15 ($n = 2$) after ischemia or on days 4 ($n = 1$) and 9 ($n = 2$) after the sham operation (Fig. 1E2; Tonchev et al., 2003a). The animals in the long-term survival group ($n = 10$) received BrdU injections on days 5–9 after surgery and were sacrificed 2, 5, and 10 weeks after the last injection, i.e., on days 23 ($n = 2$), 44 ($n = 2$), and 79 ($n = 2$) after ischemia or on days 23 ($n = 2$) and 44 ($n = 2$) after the sham operation (Fig. 2E2). The neonatal monkey received two BrdU injections, one on the day of birth and one on P14, and was euthanized 2 hr after the second injection.

Histology

The monkeys were anesthetized with lethal doses of sodium pentobarbital and intracardially perfused with 4% paraformaldehyde. The brains were removed, tissue blocks were cryoprotected in sucrose, embedded in OCT medium (Tissue-Tek, Sakura Finetech Co., Tokyo, Japan) and frozen at −70°C. Coronal (right hemisphere) or horizontal (left hemisphere) sections (40 μm thick) were cut sequentially on a cryomicrotome and stored free-floating at −20°C in a cryopreservation buffer until analysis. BrdU staining was preceded by DNA denaturation as described previously (Eriksson et al., 1998; Tonchev et al., 2003a), and incorporated BrdU was detected using mouse anti-BrdU (1:100; Becton Dickinson, San Jose, CA) or rat anti-BrdU (1:100; Harlan Sera-Lab, Loughborough, UK) antibodies. The following antibodies for phenotypic markers were applied in combination with anti-BrdU: mouse anti-Ki67 (1:50; Novocastra, Newcastle, UK), rabbit anti-phosphorylated histone H3 (1:50; Cell Signaling, Beverly, MA), rat anti-Musashi1 (1:100; Kaneko et al., 2000), rabbit anti-Musashi1 (1:200; Chemicon, Temecula, CA), rabbit or mouse anti-Nestin (1:200; Chemicon), mouse anti-neuronal nuclei (NeuN, 1:100; Chemicon), rabbit or mouse anti-β-tubulin class III (1:400; Covance, Richmond, CA), goat anti-Doublecortin (1:200; Santa Cruz Inc., Santa Cruz, CA), mouse anti-polysialylated neural cell adhesion molecule (PSA-NCAM, 1:200; a gift from Tatsunori Seki), rabbit anti-glial fibrillary acidic protein (GFAP, 1:400; Sigma), mouse anti-S100β (1:500; Sigma), rabbit anti-Iba1 (1:800; a gift from Yoshinori Imai), and rabbit anti-glutamic acid decarboxylase (GAD)65/67 (1:400; Chemicon). The rabbit antibody against Islet1 (1:400) was obtained from Chemicon and the goat anti-Tbr1 antibody (1:200) was obtained from Santa Cruz. The staining for activated caspase-3 was carried out using a rabbit anti-activated caspase-3 antibody (1:50; Cell Signaling). The primary antibodies were revealed by appropriate secondary antibodies conjugated to biotin for immunoperoxidase labeling

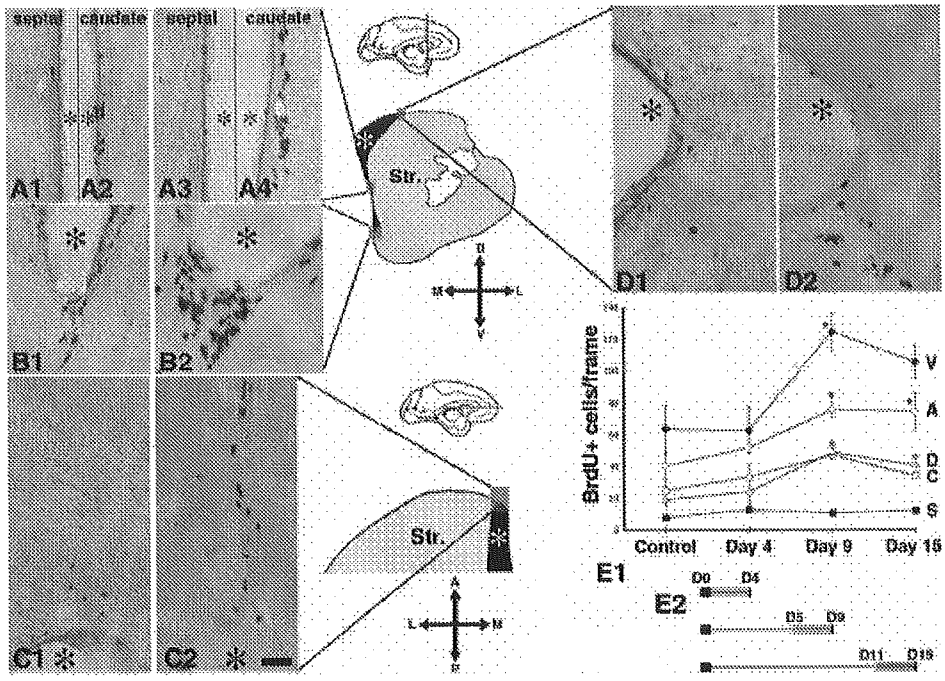

Fig. 1. Cell proliferation in the monkey group with short-term survival after BrdU. BrdU+ cells in the septal (**A1, A3**), caudate (**A2, A4**), ventral (B), dorsal (D) and anterior (C) aspects of SVZa of control (**A1, A2, B1, C1, D1**) and postischemic (**A3, A4, B2, C2, D2**) day 9 brains. M, medial; L, lateral; D, dorsal; V, ventral; A, anterior; P, posterior; Str, striatum. The lumen of the lateral ventricle is shown by an asterisk. **E1**: Quantitative evaluation of the BrdU+ cells. Note the increase in BrdU+ cells on postischemic day 9 in the ventral (V), anterior (A), dorsal (D), and caudate (C) SVZa. In contrast, no change was observed in the septal (S) SVZa. $^*P < 0.05$ vs. control animals. **E2**: BrdU infusion protocol, with gray horizontal bars depicting periods of BrdU infusion. D0, day of surgery. Scale bar = 50 μm.

(1:30–1:100, Vector ABC kit; Vector Laboratories, Burlingame, CA), or AlexaFluor 488, 546, 633 (1:100; Molecular Probes, Eugene, OR) and tetramethylrhodamine isothiocyanate (TRITC, 1:30; Jackson ImmunoResearch, West Grove, PA) for immunofluorescent labeling. For double and triple staining, the respective primary antibodies were from different species and were applied sequentially to minimize cross reactivity.

Terminal Deoxynucleotidyltransferase-Mediated UTP Nick-End Labeling Assay

Free-floating sections were subjected to the terminal deoxynucleotidyltransferase (TdT)-mediated UTP nick-end labeling (TUNEL) assay carried out using the ApopTag in situ cell death detection kit (Intergene, Purchase, NY), as described previously (Tonchev et al., 2003a). Briefly, the sections were dehydrated in an ascending ethanol/dH_2O series (50, 70, and 90%; 5 min each) followed by one 15-min incubation in 100% ethanol and rehydration in ethanol/dH_2O (90, 70, and 50%; 5 min each). Sections were then subjected to proteinase K (20 μg/mL, 15 min) followed by equilibration buffer and TdT/reaction buffer mixture at 37°C for 2 hr. Reactions involving digoxigenin incorporation were visualized by appropriate antibodies. Control stainings included DNase pretreatment (positive control for reaction specificity) or TdT omission (negative control). For TUNEL/BrdU double labeling, the reaction was developed until the enzyme step, DNA denaturation for BrdU, was carried out and then the incorporated digoxigenin and BrdU were visualized using immunostaining. For NeuN/TUNEL/BrdU triple labeling, the antibody against NeuN was applied and visualized at the end of the procedure.

Image Analysis

The numbers and densities of BrdU+ cells were determined on immunoperoxidase-labeled sections. Tissue blocks from the left hemisphere, starting dorsally at the level of the corpus callosum topping the roof of the anterior horn of the lateral ventricle and spanning ventrally until the level of the anterior commissure (ac), were cut into horizontal sections. Tissue blocks from the right hemisphere, ac+7 mm anteriorly to ac+1 mm posteriorly, were cut into coronal sections. Every 12th section was evaluated using a computerized microscope system and positive cells were displayed on a computer screen. The number of cells that had incorporated BrdU in SVZa was determined using 800 μm × 100 μm grids placed over each of the five aspects of SVZa (dorsal, ventral, septal, caudate, and anterior), as outlined on the maps in Figure 1. The BrdU+ cells in the striatum and frontal cortex were counted using 880 μm × 680 μm grids. Numbers and densities were averaged to obtain a mean density value for each region/animal group. Double and triple labeling to determine the expression of phenotypic markers and transcription factors by BrdU-expressing cells were verified using confocal laser scanning microscopy (LSM 510; Carl Zeiss, Tokyo, Japan). Alexa Fluor 488 was assigned to the green channel, TRITC or Alexa Fluor 546 were assigned to the red channel, and Alexa Fluor 633 was assigned to the blue channel. Each fluorochrome was scanned separately and sequentially to minimize the probability of signal transfer among channels. Z sectioning at intervals of 0.5–1 μm was carried out and optical stacks of at least 20 images were used for analysis. Digital three-dimensional reconstructions were created using Zeiss LSM v2.3 software. Within each region and animal group, 100 BrdU+ cells per marker were sampled for coexpression on at least five dif-

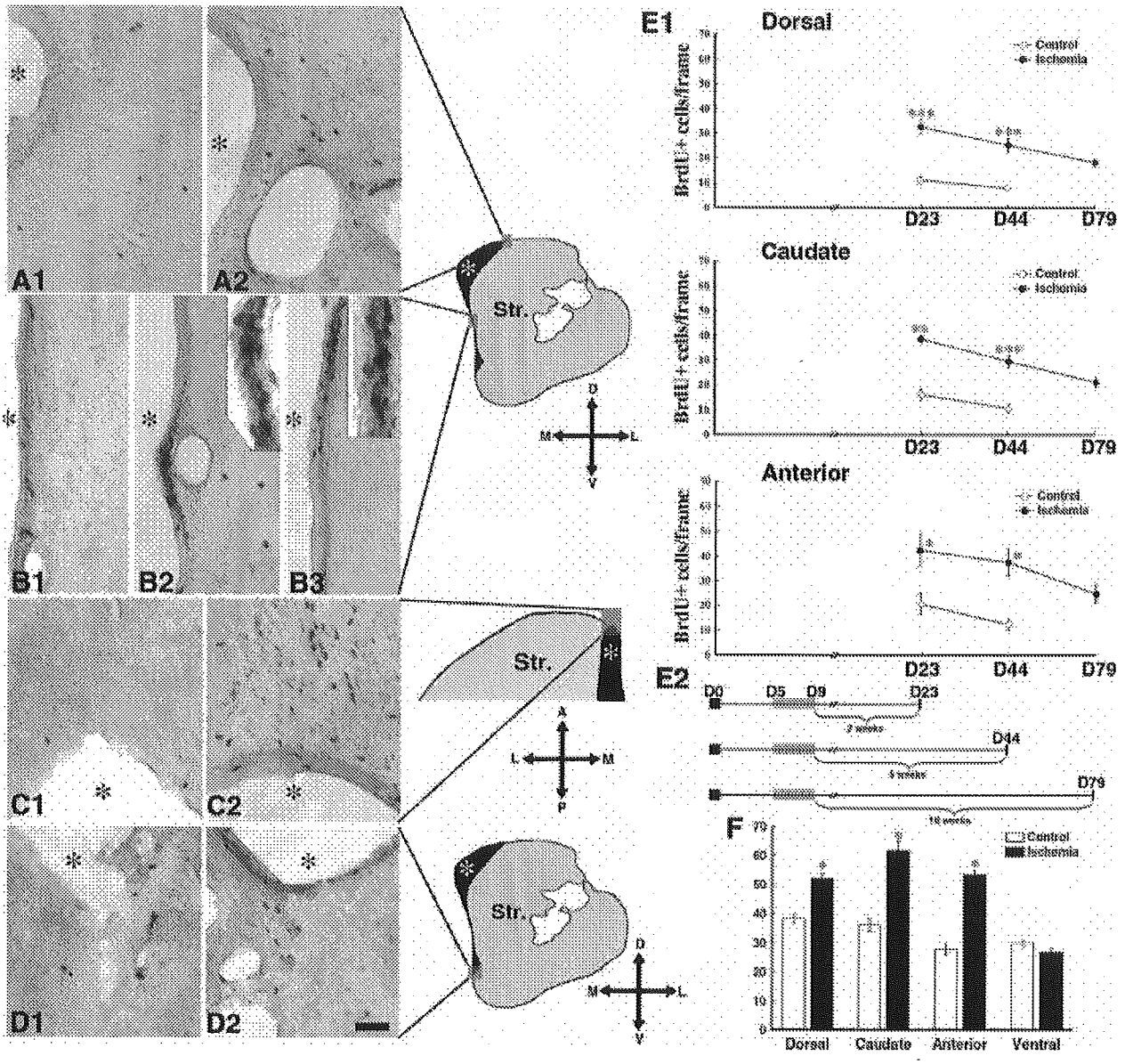

Fig. 2. Cell proliferation in the group with long-term survival after BrdU treatment. Representative images of the BrdU+ cells in the dorsal (A), caudate (B), anterior (C), and ventral (D) SVZa aspects of control day 44 (**A1, B1, C1, D1**) or postischemic day 44 (**A2, B2, C2, D2**) and day 79 (B3) brains are shown. Note the greater number of BrdU+ cells in the dorsal, caudate, or anterior SVZa aspects after ischemia. M, medial; L, lateral; D, dorsal; V, ventral; A, anterior; P, posterior; Str, striatum. The lumen of the lateral ventricle is shown by an asterisk. Scale bar = 50 μm. **E1**: Quantitative evaluation of the BrdU+ cells. The density of BrdU+ cells in the postischemic brains was significantly higher than was that of the control brains with identical survival times after BrdU treatment. $^{*}P < 0.05$, $^{***}P < 0.001$ vs. sham-operated control with the same survival time. **E2**: BrdU infusion protocol, with gray horizontal bars depicting periods of BrdU infusion. D0, day of surgery. **F**: Proportions of BrdU+ cells retaining presence in SVZa. Densities of BrdU+ cells on day 44 after sham/ischemia were calculated as a percentage of control/postischemic day 9 densities, in the presented SVZa aspects. $^{*}P < 0.05$ vs. sham-operated control.

ferent sections, whereas 200 BrdU+ cells were investigated for colabeling with NeuN.

Statistical Analysis

Data were expressed as the mean ± standard error of the mean (SEM). Differences between means were determined using one-way analysis of variance (ANOVA) followed by Tukey-Kramer's posthoc comparison and two-sided *t*-test. For comparing percentages of cells retained in SVZa, nonparametric test was also applied (Mann-Whitney). Differences were considered significant when $P < 0.05$.

RESULTS

Increased Proliferation in SVZa After Ischemia

To label de novo generated cells, we injected BrdU in ischemic or sham-operated adult macaque monkeys. We then investigated cellular proliferation in five representative locations within the SVZa (Fig. 1A–D): (1) septal SVZa along the medial wall of the lateral ventricle, (2) caudate SVZa along the lateral wall, (3) ventral SVZa at the floor of the ventricle, (4) dorsal SVZa at the roof of the ventricle capping the striatum, and (5) anterior SVZa at the rostral tip of the ventricle. In the short-term survival group, BrdU+ cells were investigated within the first 2 weeks after surgery (days 4, 9, and 15). A postischemic BrdU+ cell increase was observed in all examined aspects of SVZa except in the septal aspect, with a statistically significant peak on postischemic day 9 (Fig. 1E).

Sustained Presence of Newly Generated Cells in the Caudate, Dorsal, and Anterior Aspects of SVZa

To evaluate the long-term fate of proliferating cells in the striatum and frontal cortex, we injected BrdU during days 5–9 after surgery. Monkeys were sacrificed on days 23, 44, or 79 after ischemia or on days 23 or 44 after the sham operation (i.e., 2, 5, or 10 weeks after the last BrdU injection, respectively; Fig. 2). In the dorsal (Fig. 2A), caudate (Fig. 2B), and anterior (Fig. 2C) aspects of SVZa, the postischemic monkey brains contained more BrdU+ cells than did the respective sham-operated controls (Fig. 2E). The postischemic monkeys with BrdU survival time of 10 weeks (sacrificed on postischemic day 79) had a greater number of BrdU+ cells in the anterior, dorsal, and caudate SVZa than did the sham-operated controls with BrdU survival time of 5 weeks (24.4 ± 3.7 vs. 12.4 ± 2.4 in the anterior SVZa, 18.3 ± 1.7 vs. 8.1 ± 1.1 in the dorsal SVZa, and 21.3 ± 1.9 vs. 10.8 ± 1.7 in the caudate SVZa, respectively; $P < 0.05$, paired t-test). In ventral (Fig. 2D) and septal (data not shown) SVZa, no differences were observed between ischemic and control animals. Evaluation of the percentage of BrdU+ cells sustaining their localization in SVZa on day 44 after surgery showed significantly higher proportions of retained cells in the postischemic dorsal, caudate, and anterior SVZa, but not in ventral SVZa (Fig. 2F).

Proliferating Cells in SVZa Are Neural and Neuronal Progenitors

We confirmed that BrdU+ cells were indeed proliferating by double labeling BrdU with Ki67, a marker of cells in the G1-M phases of the cell cycle (Kee et al., 2002), and phosphorylated histone H3, an M-phase marker (Hendzel et al., 1997). We observed an almost complete colabeling of BrdU and Ki67 in SVZa of the monkeys from the short-term survival group, whereas a smaller fraction of the BrdU+ cells coexpressed phosphorylated histone H3 (Fig. 3A), consistent with our previous observation in other brain regions of these monkeys (Tonchev et al., 2003b). To determine the phenotype of proliferating cells, we utilized markers for neural (Musashi1 and Nestin) or neuronal (βIII-tubulin) progenitors (Kaneko et al., 2000; Pencea et al., 2001; Tonchev et al., 2003a). In SVZa, numerous BrdU+ cells (either single or in clusters) were double labeled for Musashi1 (Fig. 3B) and were typically negative for the astrocyte marker GFAP. We previously detected BrdU+ cells in the monkey DG and olfactory bulb that express Musashi1 and Nestin but are GFAP− (Tonchev et al., 2003a,b). As Musashi1 is expressed in both embryonic progenitors and astrocytes (Kaneko et al., 2000), the Musashi1+/BrdU+/GFAP− immunophenotype most probably represents neural progenitor cells. Consistent with such a conclusion, the same cell type also expressed Nestin (Fig. 3C). The proportion of Musashi1+/BrdU+ cells out of the total BrdU+ cells was over 70% on postischemic day 9 (Fig. 3G). At 2–10 weeks after BrdU infusion, numerous BrdU+ cells expressed the neuronal progenitor marker βIII-tubulin (Fig. 3D), whereas the proportion of Musashi1+/BrdU+ cells decreased (Fig. 3G).

Ischemia caused an increase of cells positive for the TUNEL assay in the striatum and neocortex (Supplementary Fig. 1); however, BrdU+ cells never colabeled with either TUNEL or with active caspase-3, a marker of apoptotic cells (Fig. 3E). Furthermore, we observed Musashi1+/BrdU+ progenitors coexpressing Ki67 not only in the short-term survival group but also the long-term survival group, as late as postischemic day 79 (Fig. 3F).

Fig. 3. Expression of proliferation and progenitor cell markers by BrdU+ cells. **A:** Triple labeling for phosphorylated histone H3 (pHis3), Ki67, and BrdU in postischemic day 9 SVZa. The boxed area in **A1** is shown in **A2** with color separation. **B:** Triple immunostaining for Musashi1, glial fibrillary acidic protein (GFAP) and BrdU in postischemic day 9 SVZa. A Musahsi1+/BrdU+ cluster (arrow in **B1**) is GFAP−, as confirmed by 3D reconstruction (the x- and y-planes are on the right and top, respectively) and shown with color separation in **B2**. **C:** Triple labeling for Nestin, Musashi1, and BrdU shows a proliferating cell cluster (arrow) expressing both Musashi1 and Nestin in postischemic day 9 SVZa. The cluster in **A1** is shown in **A2** with color separation. **D:** Double immunofluorescence for βIII-tubulin and BrdU in postischemic day 23 SVZa. The boxed area in **D2** is shown in **D3** with color separation. **E:** Double labeling for BrdU/TUNEL (**E1, E2**) or BrdU/active caspase-3 (**E3, E4**) in postischemic day 9 (**E1, E3**) or day 79 (**E2, E4**) SVZa. BrdU+ cells (red) are depicted by arrows, whereas TUNEL+ or Caspase+ cells (green) are shown by arrowheads. **F:** Triple immunofluorescence for Musashi1, Ki67, and BrdU in postischemic day 79 SVZa. A triple-stained cell is depicted by arrows, and a BrdU+/Ki67+/Musashi1− cell is depicted by arrowheads. The lumen of the lateral ventricle is shown by an asterisk. **G:** Proportions of BrdU+ cells coexpressing Musashi1 or βIII-tubulin in SVZa (BrdU+ cells were sampled in dorsal, caudate, ventral, and anterior aspects) of postischemic monkeys. BrdU+/Musashi1−/βIII-tubulin− cells are designated "other." Scale bar = 50 μm in B1 (for **A1, B1**); 20 μm in **A2, B2, C1,** and **D2** (for **D1** and **D2**); 10 μm in **C2, D3,** and **E1** (for **E1–E4**); and 5 μm in **F1** (for **F1–F4**).

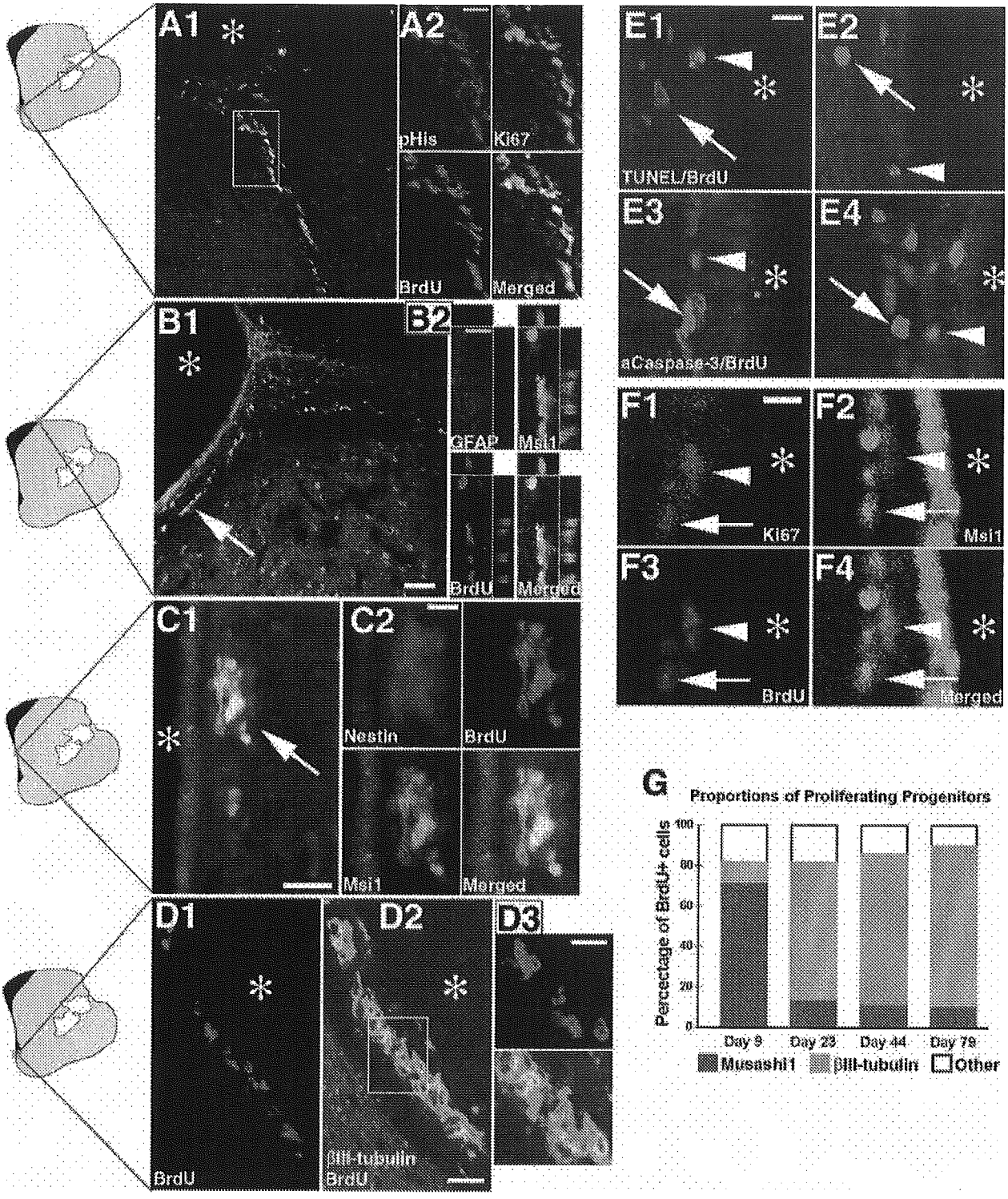
A1
A2
pHis
Ki67
BrdU
Merged
B1
B2
GFAP
Msi1
BrdU
Merged
C1
C2
Nestin
BrdU
Msi1
Merged
D1
D2
D3
BrdU
βIII-tubulin
BrdU
E1
E2
TUNEL/BrdU
E3
E4
aCaspase-3/BrdU
F1
F2
Ki67
Msi1
F3
F4
BrdU
Merged
G
Proportions of Proliferating Progenitors
Percentage of BrdU+ cells
100
80
60
40
20
0
Day 9
Day 23
Day 44
Day 79
Musashi1
βIII-tubulin
Other

Figure 3.

SVZa Progenitor Migration Is Restricted Along a Pathway to the Olfactory Bulb

The postischemic enhancement of progenitor proliferation in SVZa might potentially lead to the migration of newly generated cells to either the olfactory bulb along a pathway known as the rostral migratory stream (RMS; Iwai et al., 2003) or to other brain regions, as demonstrated in rodent models of focal cerebral ischemia in the neocortex (Zhang et al., 2001; Jin et al., 2003) or striatum (Arvidsson et al., 2002; Parent et al., 2002). We therefore investigated whether any of these possible migration pathways existed in postischemic monkey brains.

As the ventral aspect of the SVZa had the highest density of BrdU+ cells, we investigated the white matter located ventrally to SVZa. On sections stained for BrdU alone, we found chains of BrdU+ cells that were particularly dense in the monkey brains with short-term survival after BrdU treatment and that gradually became less populated by BrdU+ cells in the long-term survival brains (Fig. 4A). The BrdU+ cells within these chains, apparently part of the "ventral extension of SVZ" (Pencea et al., 2001) that together with RMS contributes to olfactory bulb neurogenesis, did not deviate away from the chains toward adjacent telencephalic structures (Fig. 4A). BrdU+ chains of cells were not observed in the subcortical white matter on the dorsal aspect of the SVZa (data not shown).

We applied βIII-tubulin/BrdU immunohistochemistry followed by confocal analysis to investigate whether migration of immature neurons may take place in postischemic monkey brain. We found no evidence for either βIII-tubulin+/BrdU+ cells or for βIII-tubulin+ chains in the white matter between the lateral ventricle and the prefrontal neocortex or along the border between the white matter and the striatal edge of ischemic monkey brain (Fig. 4C). Because this negative result could have been caused by an inadequacy of our protocol, we tested the reliability of our immunohistochemistry procedure using brain sections from a neonatal monkey that had been injected with BrdU on the day of birth and on P14, and then sacrificed 2 hr later. The brain sections from the P14 monkey were processed simultaneously with the sections from the adult monkeys. Staining for βIII-tubulin revealed numerous βIII-tubulin+ clusters in the white matter adjacent to the prefrontal neocortex (Fig. 4B), some of which were double labeled for BrdU (inset in Fig. 4B). Identical results were obtained with two independent markers of migrating immature neurons, PSA-NCAM (Seki and Arai, 1993) or Doublecortin (Gleeson et al., 1999; Supplementary Fig. 2).

In the rostral migratory stream (Fig. 4D), we found numerous βIII-tubulin+/BrdU+ cells that were typically arranged in chains similar to the BrdU+ cells in the ventral portions of the SVZa. The lack of evidence for SVZa progenitor cell migration outside the RMS to the olfactory bulb combined with the lack of data for the apoptosis of newly generated cells (Fig. 3E) suggests that ischemia likely increases the number of BrdU+ cells in RMS and the olfactory bulb. Consistent with this notion, we found an increased number of BrdU+ cells along the postischemic RMS at postischemic day 23 (2 weeks after BrdU), compared to that in the sham-operated controls (Fig. 4E) with the same survival time after BrdU treatment (158.8 ± 25.1 vs. 54.1 ± 9.3 BrdU+ cells/mm^2; $P < 0.05$, paired t-test). In addition, an increased number of BrdU+ cells existed in the postischemic olfactory bulbs of the monkey group with a 5-week survival period after BrdU treatment (postischemic day 44) compared to that in the olfactory bulbs of sham-operated monkeys (Fig. 4F) with the same survival time (59.5 ± 8.8 vs. 33.1 ± 2.4 BrdU+ cells/mm^2; $P < 0.05$, paired t-test).

Predominant Glial Cell Proliferation in Postischemic Striatum and Neocortex

Similar to the situation in the SVZa, the ischemic insult enhanced proliferation in the striatum and frontal cortex; in both of these regions, the density of BrdU+ cells on postischemic day 9 was markedly higher than that in the control group (Fig. 5A). Among the monkeys from the long-term survival group, the BrdU+ cells in the postischemic striatum and frontal cortex significantly outnumbered those in the control monkeys at both 2 and 5 weeks after BrdU treatment (Fig. 5B). Similarly to SVZa, the postischemic macaques with a BrdU survival time of 10 weeks (postischemic day 79) had a greater number of BrdU+ cells than did the sham-operated controls with a BrdU survival time of 5 weeks in both regions of interest (35.4 ± 3.7 vs. 19.7 ± 2.6 in the striatum and 40.4 ± 9.4 vs. 14.9 ± 1.8 in the neocortex; $P < 0.05$, paired t-test).

Numerous BrdU+ cells expressed the microglial marker Iba1 (Ito et al., 1998; Fig. 5C) and the astroglial markers S100β (Fig. 5D) and GFAP (data not shown). Double labeling with BrdU revealed that a stable proportion of about 90% of the newly generated cells in the two regions after ischemia were glia (Fig. 5E). Microglial cells were much more numerous than astrocytes were, by approximately 8:1 (Fig. 5D,E). Astroglia were found frequently in proliferating "doublets" (data not shown), as described previously in the postischemic monkey hippocampus and temporal neocortex (Tonchev et al., 2003a). Perineuronal satellite cells did not express either microglial or astroglial markers (Fig. 5C).

Limited Neuronal Production in the Postischemic Striatum and Neocortex

We searched for evidence of de novo generation of cells with a neuronal immunophenotype in the striatum and frontal cortex because these regions were reported previously to contain such cells in normal monkeys (Gould et al., 2001; Bedard et al., 2002). We first carried out double staining for BrdU and the mature neuronal

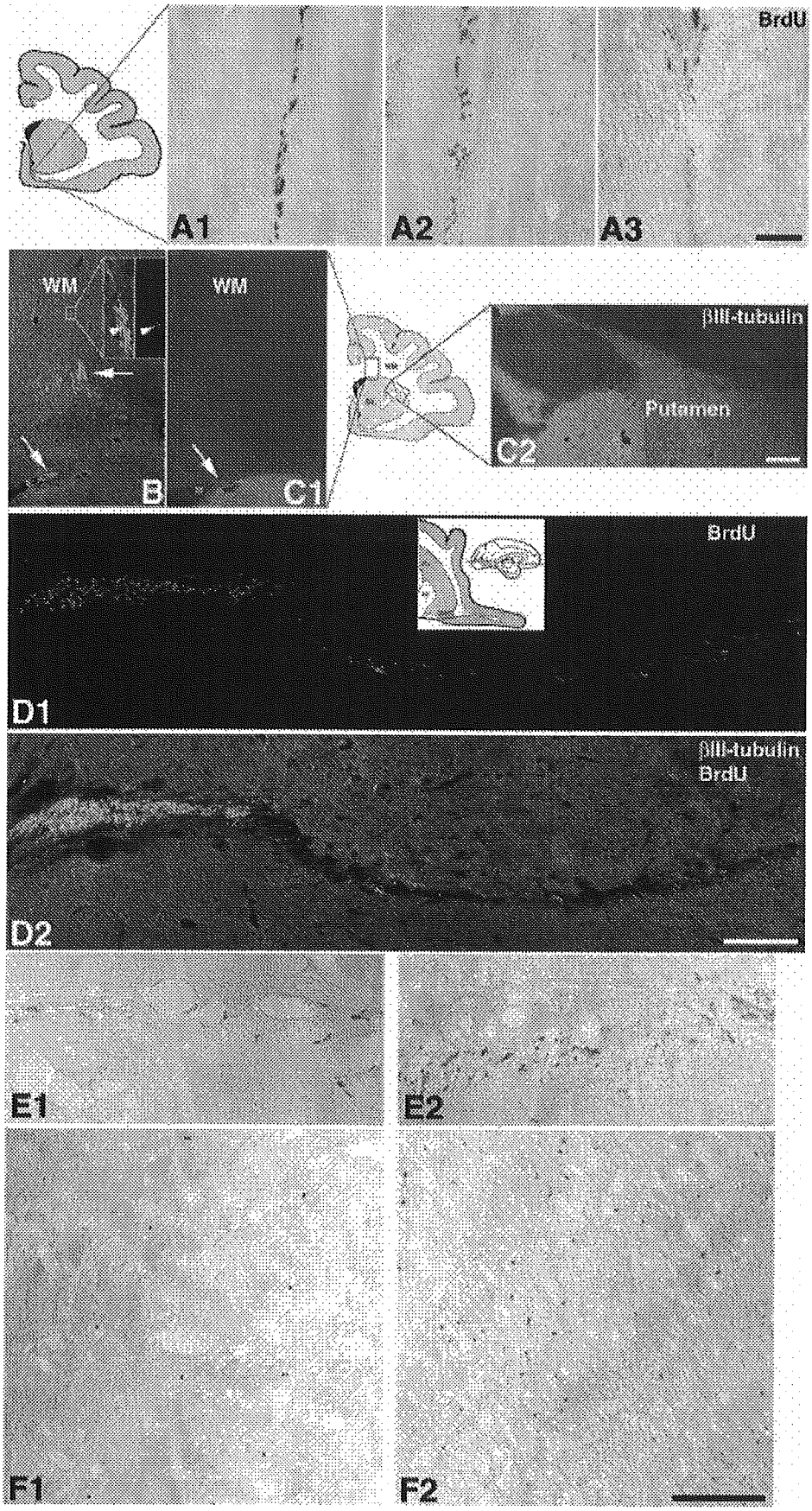

Fig. 4. Proliferation of progenitor cells in the macaque rostral migratory stream (RMS) and subcortical white matter. **A:** BrdU immunohistochemistry in the white matter located ventral to the ventral aspect of SVZa on postischemic days 9 (**A1**), 15 (**A2**), and 44 (**A3**). Note the stream of BrdU+ cells and the lack of cells deviating away from the stream. **B, C**: Staining for βIII-tubulin in the subcortical white matter and in the vicinity of the putamen of an intact postnatal (**B**) and adult postischemic day 23 (**C1, C2**) monkey brain. Note the lack of positive cells in the adult monkey white matter contrasting the numerous βIII-tubulin+ clusters (arrows in **B**) in the postnatal (P14) brain. The boxed cluster is magnified in the inset with arrowheads depicting a βIII-tubulin+/BrdU+ cell. Cells positive for βIII-tubulin in SVZa are also shown (arrows). WM, white matter; Str, striatum; F, frontal cortex. The lumen of the lateral ventricle is shown by an asterisk. **D:** Double labeling for βIII-tubulin and BrdU in control and postischemic monkey RMS (horizontal brain sections at the level of the anterior commissure), 23 days after surgery. Virtually all BrdU+ cells are colocalized with βIII-tubulin; none of the cells positive for either marker deviate away from the RMS. Pu, putamen; ac, anterior commissure. **E:** BrdU immunohistochemistry in RMS of a control (**E1**) and postischemic day 23 (**E2**) monkey. **F:** BrdU immunohistochemistry in the olfactory bulb parenchyma of a control (**F1**) and postischemic day 44 (**F2**) monkey. Scale bar = 400 μm in **A3** (for **A1–A3**); 400 μm in **C2** (for **B, C, C2**); 200 μm in **D2** (for **D1, D2**); and 200 μm in **F2** (for **E, F**).

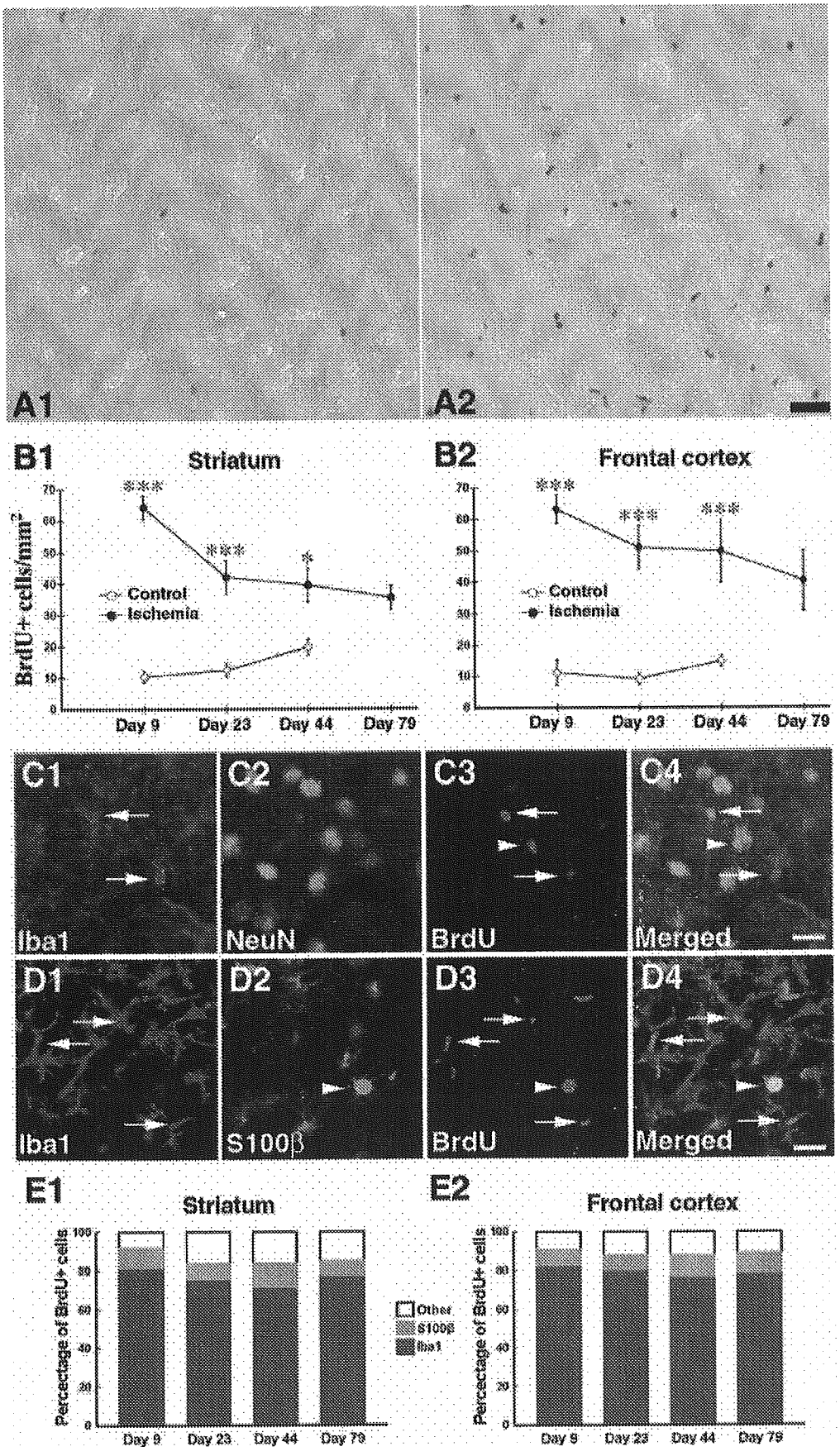

Fig. 5. Cell proliferation in the striatum and frontal cortex. **A:** Representative images of BrdU+ cells in the striatum of control (**A1**) and postischemic day 9 monkey brains (**A2**). Note the greatly increased density of BrdU+ cells on day 9. **B:** Quantitative evaluation of the BrdU+ cells in striatum (**B1**) and frontal cortex (**B2**) at various intervals after ischemia/sham operation. The density of BrdU+ cells in the postischemic brains is significantly greater than that in the control brains with identical survival periods after BrdU treatment. $*P < 0.05$, $***P < 0.001$ vs. control animals. **C:** Triple labeling for Iba1, NeuN, and BrdU in the postischemic day 44 striatum. Iba1+/BrdU+ cells are indicated by arrows, whereas a perineuronal satellite cell is indicated by an arrowhead. **D**: Triple labeling for Iba1, S100β, and BrdU in the postischemic day 44 frontal cortex. Iba1+/BrdU+ cells (arrows) are much more numerous than are the S100β+/BrdU+ cells (arrowhead). **E**: Proportions of BrdU+ cells coexpressing Iba1 or S100β in the postischemic monkeys. BrdU+/Iba1−/S100β− cells are designated "other." Scale bar = 50 μm in **A**; 20 μm in **C, D**; 10 μm in **E, F**.

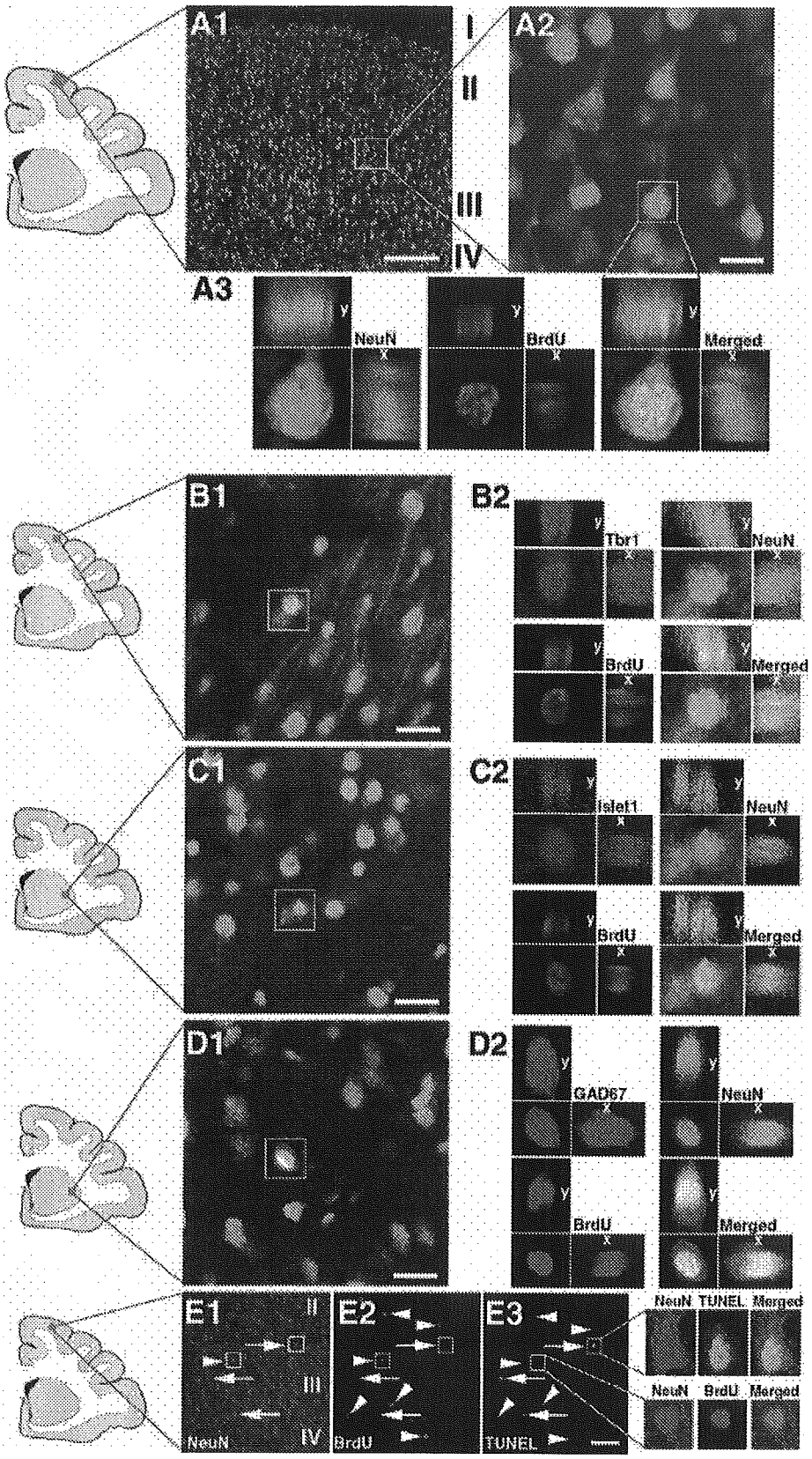

Fig. 6. Neuronal immunophenotype of BrdU+ cells in the postischemic neocortical or striatal parenchyma. **A:** Double labeling for NeuN and BrdU in neocortical layers I–IV (**A1**) reveals a double-labeled cell at the boundary of layers II and III (the box in **A1** is magnified in **A2**) on postischemic day 23. The cell boxed in **A2** is presented as orthogonal projections along the x- and y-axes (**A3**) to confirm the colocalization of the two signals. Note its identical morphology to neighboring Neu N+/BrdU− cells (**A2**). **B:** Triple labeling for BrdU, NeuN, and Tbr1 at the boundary of neocortical layers IV and V on day 44. The boxed cell in **B1** is shown in **B2** with color separation and orthogonal projections. **C:** Triple labeling for BrdU, NeuN and Islet1 in the putamen on day 44. The boxed cell in **C1** is shown in **C2** with color separation and orthogonal projections. **D:** Triple-labeling for BrdU, NeuN, and the GAD67 in the putamen on day 79. The boxed cell in **D1** is shown in **D2** with color separation and orthogonal projections. **E:** Triple staining for NeuN (**E1**), BrdU (**E2**) and TUNEL (**E3**) in layers II-IV of the neocortex on postischemic day 23. TUNEL+ cells (arrows) and the BrdU+ cells (arrowheads) are distinct cell types. Examples of a NeuN+/TUNEL+ cell and a NeuN+/BrdU+ cell boxed in **E1-E3** are magnified on the right side of the figure. Scale bar = 200 μm in **A1**; 20 μm in **A2, B1, C1** and **D1**; 50 μm in **E1–E3**.

marker NeuN (Eriksson et al., 1998; Gould et al. 1999b, 2001; Kornack and Rakic, 1999, 2001b; Arvidsson et al., 2002; Parent et al., 2002), searching for double-labeled cells whose size and morphology were similar to the surrounding NeuN+/BrdU− neurons (Fig. 6A). A systematic confocal analysis revealed that a few of the BrdU+ cells were NeuN+/BrdU+ cells: 8/600 in the neocortex (2/200 at day 23, 3/200 at day 44, and 3/200 at day 79) and 7/600 in the striatum (2/200 at day 23, 3/200 at day 44, and 2/200 at day 79).

We further confirmed the putative neuronal phenotype of the NeuN+/BrdU+ cells by demonstrating that they express markers of committed neuronal progenitors and postmitotic neurons in the striatum (Islet1; Stenman et al., 2003) or the neocortex (Tbr1; Englund et al., 2005). In addition to the 1,200 BrdU+ cells examined for NeuN/BrdU double labeling as described above, we investigated 300 BrdU+ cells (100 in each of the postischemic groups sacrificed on days 23, 44, and 79) for Tbr1/NeuN/BrdU triple labeling in the neocortex and 300 BrdU+ cells for Islet1/NeuN/BrdU triple labeling in the striatum. Three-dimensional confocal analysis with digital reconstructions demonstrated that all scanned NeuN+/BrdU+ cells coexpressed Tbr1 in the neocortex (4/300; Fig. 6B) or Islet1 in the striatum (5/300; Fig. 6C). Finally, we found that the NeuN+/BrdU+ cells coexpressed GAD, a marker of γ-aminobutyric acid (GABA)ergic neurons (Jongen-Relo et al., 1999). We observed triple-labeled GAD+/NeuN+/BrdU+ cells in both the striatum (2/200 BrdU+ cells; Fig. 6D) and neocortex (2/200 BrdU+ cells). In the sham-operated monkeys, BrdU+/NeuN+ cells were only observed in striatum and neocortex of the day 44 brains (1/200 BrdU+ cells).

In a rodent ischemic model, BrdU incorporation in neurons was shown to precede their apoptosis, as revealed by positive TUNEL staining (Kuan et al., 2004). Combining BrdU/TUNEL double labeling with NeuN immunohistochemistry in the striatum and neocortex of postischemic day 23 monkeys, we found no TUNEL+/NeuN+ cells incorporating BrdU, and all NeuN+/BrdU+ cells remained negative for TUNEL (Fig. 6E).

DISCUSSION

The present study has 3 major findings: (1) the enhanced and sustained presence of progenitors in SVZa, particularly after ischemia; (2) the restriction of migration of progenitor cells away from SVZa toward the olfactory bulb, but not toward the postischemic striatum or frontal cortex; and (3) the ability of the adult primate brain to sustain striatal and neocortical neuronal production after a global ischemic insult.

We have demonstrated previously that global ischemia in adult macaque monkeys increases the progenitor cell proliferation in the SVZ along the inferior horn of the lateral ventricle (SVZi; Tonchev et al., 2003a). Here, we extend those results by investigating the SVZ along the anterior horn of the lateral ventricle (SVZa). Our results demonstrate for the first time that in primates, global cerebral ischemia enhances cell proliferation in this region. The presence of SVZa progenitor cells in normal adult macaque monkeys has been reported in a previous study (Kornack and Rakic, 2001a). The present study, however, demonstrates the first quantitative analysis of the BrdU+ cells that persist in SVZ for a long time. The data indicate that although SVZa progenitors sustain their presence in SVZa of both control and ischemic monkeys, postischemic SVZa retained a significantly higher proportion of progenitor cells than did control SVZa (Fig. 2F). In addition, long-term BrdU-retaining cells expressed Musashi1 and Ki67, indicating they remained uncommitted to neuronal or glial lineage neural progenitors in the active phases of their cell cycle. Interestingly, a subpopulation of stem cells implanted in the lateral ventricles of embryonic monkeys retained their location in SVZa 4 weeks after implantation, exhibiting features of undifferentiated progenitors (Ourednik et al., 2001). Our results extend these findings by demonstrating the potential of the endogenous SVZa progenitors of the adult monkey brain to retain their location in the niche, particularly after injury.

The finding of long-term BrdU-retaining cells in SVZa can be explained as follows. First, we specifically used a high BrdU dose (five daily injections of 100 mg/kg each) in an attempt to diminish the possibility of BrdU label dilution by cell division, with a resulting loss in BrdU detection using immunohistochemistry. A high BrdU dose should guarantee BrdU detection throughout long-term survival periods, especially because turnover of some adult-generated cells in the monkey brain is not rapid (Kornack and Rakic, 2001a; Gould et al., 2001). Second, in rodents, stem cells residing in SVZa have the ability to exit and then reenter the cell cycle (Maslov et al., 2004). If some primate progenitors possessed a similar ability, the long-term BrdU label-retaining cells in the SVZa that are colabeled by Ki67 might represent precursor cells or their progeny reentering the cell cycle. Third, the retention of SVZa progenitors might be due to a lack of migration or differentiation signals or, alternatively, to an enhanced signal maintaining the stem/progenitor phenotype. The molecular nature of such putative signals in the primate remains to be elucidated. Fourth, long-term BrdU-label retaining cells might represent a pathologic, abnormal, state. These cells remained negative for markers of DNA damage and apoptosis, TUNEL and active caspase-3, however, arguing against this latter possibility.

In rodent focal ischemic models, SVZa emerged as the main source of precursor cells for neuronal production in the striatum and cortex (Zhang et al., 2001, 2004; Arvidsson et al., 2002; Parent et al., 2002; Jin et al., 2003). Different from these rodent focal ischemic models, however, in adult primate brains after global ischemia we failed to find evidence that SVZa contributes to the generation of striatal or neocortical neurons. Although we observed chains of proliferating neuronal

progenitors in the RMS migrating toward the olfactory bulb, no such "stream" (Gould et al., 1999b, 2001) was evident in the subcortical white matter. In comparison, in the early postnatal (P14) monkey brain, we found numerous nests of immature neurons in the subcortical white matter. We observed a significantly increased proliferation in RMS at 2 weeks after BrdU treatment (day 23) and in the olfactory bulb parenchyma at 5 weeks after BrdU treatment (day 44). Such results are consistent with the notion that the postischemia-generated SVZa precursor cells are directed selectively toward the olfactory bulb. Notably, however, our model of transient global ischemia caused a less pronounced injury (Yoshida et al., 2002) than did the large focal injury induced in the rat stroke models (Zhang et al., 2001, 2004; Arvidsson et al., 2002; Parent et al., 2002; Jin et al., 2003). The differences in progenitor cell migration thus might be related to the strength of the insult, i.e., a milder ischemic insult might be unable to trigger progenitor cell migration toward the postischemic striatum or cortex. Application of a monkey focal ischemic model in future studies would be important to define more precisely the ability of primate progenitors to respond to stroke.

Despite the lack of evident progenitor migration toward the postischemic neocortex or striatum, we investigated a total of 2,200 BrdU+ cells in these two regions and found 28 that were colabeled by NeuN (slightly over 1% of the BrdU+ cells examined). These putative newly generated neurons survived for up to 70 days after BrdU treatment (79 days after ischemia) and remained a stable proportion of the BrdU+ cells in the cortex and striatum of the monkeys, with long-term survival after BrdU treatment. In contrast, newly generated neurons in normal monkey neocortex have a transient existence (Gould et al., 2001). We have provided three lines of evidence supporting our identification of adult-generated neurons in the monkey neocortex and striatum: (1) we observed NeuN+/BrdU+ cells that were morphologically identical to neighboring NeuN+/BrdU− neurons; (2) the NeuN+/BrdU+ cells expressed region-specific transcription factors expressed by neuronal progenitors during their transition into postmitotic neurons and in postmitotic neurons themselves, namely Islet1 in the striatum (Stenman et al., 2003) and Tbr1 in the neocortex (Englund et al., 2005); and (3) the NeuN+/BrdU+ cells expressed the enzyme GAD and therefore could be GABAergic interneurons, consistent with their preferential localization in neocortical layers II–IV.

Recently, ischemia was shown to induce BrdU incorporation in dying neurons before apoptosis, as revealed by positive TUNEL staining (Kuan et al., 2004). The dying neurons gradually disappeared by postischemic day 28, whereas BrdU+ cells with a neuronal morphology were observed at later time points (days 44 and 79) in the present study. We also demonstrated that in the striatum and neocortex on postischemic day 23, BrdU was not incorporated in TUNEL+/NeuN+ cells and that NeuN+/BrdU+ cells remained negative for TUNEL (Fig. 6E). These results indicate that in our model and under the current BrdU protocol, the NeuN+/BrdU+ cells we described were not dying neurons with aberrant DNA synthesis. This is consistent with our findings in the postischemic monkey hippocampal CA1 sector (Tonchev et al., 2003a).

Our data suggests the possibility that newly generated neocortical and striatal neurons might arise from parenchymal progenitors. Previous findings in primates are in accordance with such a conclusion: (1) the in vitro isolation of progenitor cells from adult human gray and white matter (Arsenijevic et al., 2001; Nunes et al., 2003); and (2) the observation that a small fraction of neural stem cells migrating from the SVZa to the developing monkey neocortex remain undifferentiated in the brain parenchyma (Ourednik et al., 2001) and thus could remain dormant during development into adulthood until activated by injury. Very recently, Dayer et al. (2005) provided in vivo evidence in adult rodents that at least in the neocortex, GABAergic interneurons might be generated by a local pool of precursors.

A more detailed understanding of the molecular mechanisms controlling adult primate progenitors may provide an important insight into their manipulation in situ (Magavi et al., 2000) to restore neurologic function in human disease as well as in deciphering species- and age-selective differences in their behavior.

ACKNOWLEDGMENTS

The present research was supported by a Grant-in-Aid for Scientific Research (Kiban-Kennkyu [B]) from the Japanese Ministry of Education, Culture, Sports, Science and Technology and from the National Science Fund of Bulgaria (L1311/03).

We thank Y. Imai (National Institute of Neuroscience, Tokyo, Japan) for the anti-Iba1 antibody, T. Seki (Juntendo University, Tokyo, Japan) for the anti-PSA-NCAM antibody, and G. Chaldakov for valuable assistance.

REFERENCES

Arsenijevic Y, Villemure JG, Brunet JF, Bloch JJ, Deglon N, Kostic C, Zurn A, Aebischer P. 2001. Isolation of multipotent neural precursors residing in the cortex of the adult human brain. Exp Neurol 170:48–62.

Arvidsson A, Collin T, Kirik D, Kokaia Z, Lindvall O. 2002. Neuronal replacement from endogenous precursors in the adult brain after stroke. Nat Med 8:963–970.

Bedard A, Cossette M, Levesque M, Parent A. 2002. Proliferating cells can differentiate into neurons in the striatum of normal adult monkey. Neurosci Lett 328:213–216.

Dayer AG, Cleaver KM, Abouantoun T, Cameron HA. 2005. GABAergic interneurons in the adult neocortex and striatum are generated from different precursors. J Cell Biol 168:415–427.

Englund C, Fink A, Lau C, Pham D, Daza RA, Bulfone A, Kowalczyk T, Hevner RF. 2005. Pax6, Tbr2, and Tbr1 are expressed sequentially by radial glia, intermediate progenitor cells, and postmitotic neurons in developing neocortex. J Neurosci 25:247–251.

Eriksson PS, Perfilieva E, Bjork-Eriksson T, Alborn AM, Nordborg C, Peterson DA, Gage FH. 1998. Neurogenesis in the adult human hippocampus. Nat Med 4:1313–1317.

Gage FH. 2000. Mammalian neural stem cells. Science 287:1433–1438.

Gleeson JG, Lin PT, Flanagan LA, Walsh CA. 1999. Doublecortin is a microtubule-associated protein and is expressed widely by migrating neurons. Neuron 23:257–271.

Gould E, Reeves AJ, Fallah M, Tanapat P, Gross CG, Fuchs E. 1999a. Hippocampal neurogenesis in adult Old World primates. Proc Natl Acad Sci USA 96:5263–5267.

Gould E, Reeves AJ, Graziano MS, Gross CG. 1999b. Neurogenesis in the neocortex of adult primates. Science 286:548–552.

Gould E, Vail N, Wagers M, Gross CG. 2001. Adult-generated hippocampal and neocortical neurons in macaques have a transient existence. Proc Natl Acad Sci USA 98:10910–10917.

Gu W, Brannstrom T, Wester P. 2000. Cortical neurogenesis in adult rats after reversible photothrombotic stroke. J Cereb Blood Flow Metab 20:1166–1173.

Hendzel MJ, Wei Y, Mancini MA, Van Hooser A, Ranalli T, Brinkley BR, Bazett-Jones DP, Allis CD. 1997. Mitosis-specific phosphorylation of histone H3 initiates primarily within pericentromeric heterochromatin during G2 and spreads in an ordered fashion coincident with mitotic chromosome condensation. Chromosoma 106:348–360.

Ito D, Imai Y, Ohsawa K, Nakajima K, Fukuuchi Y, Kohsaka S. 1998. Microglia-specific localization of a novel calcium binding protein, Iba1. Brain Res Mol Brain Res 57:1–9.

Iwai M, Sato K, Kamada H, Omori N, Nagano I, Shoji M, Abe K. 2003. Temporal profile of stem cell division, migration, and differentiation from subventricular zone to olfactory bulb after transient forebrain ischemia in gerbils. J Cereb Blood Flow Metab 23:331–341.

Jin K, Minami M, Lan JQ, Mao XO, Batteur S, Simon RP, Greenberg DA. 2001. Neurogenesis in dentate subgranular zone and rostral subventricular zone after focal cerebral ischemia in the rat. Proc Natl Acad Sci USA 98:4710–4715.

Jin K, Sun Y, Xie L, Peel A, Mao XO, Batteur S, Greenberg DA. 2003. Directed migration of neuronal precursors into the ischemic cerebral cortex and striatum. Mol Cell Neurosci 24:171–189.

Jongen-Relo AL, Pitkanen A, Amaral DG. 1999. Distribution of GABAergic cells and fibers in the hippocampal formation of the macaque monkey: an immunohistochemical and in situ hybridization study. J Comp Neurol 408:237–271.

Kaneko Y, Sakakibara S, Imai T, Suzuki A, Nakamura Y, Sawamoto K, Ogawa Y, Toyama Y, Miyata T, Okano H. 2000. Musashi1: an evolutionally conserved marker for CNS progenitor cells including neural stem cells. Dev Neurosci 22:139–153.

Kee NJ, Preston E, Wojtowicz JM. 2001. Enhanced neurogenesis after transient global ischemia in the dentate gyrus of the rat. Exp Brain Res 136:313–320.

Kee N, Sivalingam S, Boonstra R, Wojtowicz JM. 2002. The utility of Ki-67 and BrdU as proliferative markers of adult neurogenesis. J Neurosci Methods 115:97–105.

Koketsu D, Mikami A, Miyamoto Y, Hisatsune T. 2003. Nonrenewal of neurons in the cerebral neocortex of adult macaque monkeys. J Neurosci 23:937–942.

Kornack DR, Rakic P. 1999. Continuation of neurogenesis in the hippocampus of the adult macaque monkey. Proc Natl Acad Sci USA 96:5768–5773.

Kornack DR, Rakic P. 2001a. The generation, migration, and differentiation of olfactory neurons in the adult primate brain. Proc Natl Acad Sci USA 98:4752–4757.

Kornack DR, Rakic P. 2001b. Cell proliferation without neurogenesis in adult primate neocortex. Science 294:2127–2130.

Kuan CY, Schloemer AJ, Lu A, Burns KA, Weng WL, Williams MT, Strauss KI, Vorhees CV, Flavell RA, Davis RJ, Sharp FR, Rakic P. 2004. Hypoxia-ischemia induces DNA synthesis without cell proliferation in dying neurons in adult rodent brain. J Neurosci 24:10763–10772.

Liu J, Solway K, Messing RO, Sharp FR. 1998. Increased neurogenesis in the dentate gyrus after transient global ischemia in gerbils. J Neurosci 18:7768–7778.

Magavi SS, Leavitt BR, Macklis JD. 2000. Induction of neurogenesis in the neocortex of adult mice. Nature 405:951–955.

Maslov AY, Barone TA, Plunkett RJ, Pruitt SC. 2004. Neural stem cell detection, characterization, and age-related changes in the subventricular zone of mice. J Neurosci 24:1726–1733.

Nakatomi H, Kuriu T, Okabe S, Yamamoto S, Hatano O, Kawahara N, Tamura A, Kirino T, Nakafuku M. 2002. Regeneration of hippocampal pyramidal neurons after ischemic brain injury by recruitment of endogenous neural progenitors. Cell 110:429–441.

Nunes MC, Roy NS, Keyoung HM, Goodman RR, McKhann G 2nd, Jiang L, Kang J, Nedergaard M, Goldman SA. 2003. Identification and isolation of multipotential neural progenitor cells from the subcortical white matter of the adult human brain. Nat Med 9:439–447.

Ourednik V, Ourednik J, Flax JD, Zawada WM, Hutt C, Yang C, Park KI, Kim SU, Sidman RL, Freed CR, Snyder EY. 2001. Segregation of human neural stem cells in the developing primate forebrain. Science 293:1820–1824.

Parent JM, Vexler ZS, Gong C, Derugin N, Ferriero DM. 2002. Rat forebrain neurogenesis and striatal neuron replacement after focal stroke. Ann Neurol 52:802–813.

Pencea V, Bingaman KD, Freedman LJ, Luskin MB. 2001. Neurogenesis in the subventricular zone and rostral migratory stream of the neonatal and adult primate forebrain. Exp Neurol 172:1–16.

Seki T, Arai Y. 1993. Distribution and possible roles of the highly polysialylated neural cell adhesion molecule (NCAM-H) in the developing and adult central nervous system. Neurosci Res 17:265–290.

Stenman J, Toresson H, Campbell K. 2003. Identification of two distinct progenitor populations in the lateral ganglionic eminence: implications for striatal and olfactory bulb neurogenesis. J Neurosci 23:167–174.

Tonchev AB, Yamashima T, Zhao L, Okano HJ, Okano H. 2003a. Proliferation of neural and neuronal progenitors after global brain ischemia in young adult macaque monkeys. Mol Cell Neurosci 23:292–301.

Tonchev AB, Yamashima T, Zhao L, Okano H. 2003b. Differential proliferative response in the postischemic hippocampus, temporal cortex and olfactory bulb of young adult macaque monkeys. Glia 42:209–224.

Yagita Y, Kitagawa K, Ohtsuki T, Takasawa KI, Miyata T, Okano H, Hori M, Matsumoto M. 2001. Neurogenesis by progenitor cells in the ischemic adult rat hippocampus. Stroke 32:1890–1896.

Yamashima T, Kohda Y, Tsuchiya K, Ueno T, Yamashita J, Yoshioka T, Kominami E. 1998. Inhibition of ischaemic hippocampal neuronal death in primates with cathepsin B inhibitor CA-074: a novel strategy for neuroprotection based on "calpain-cathepsin hypothesis." Eur J Neurosci 10:1723–1733.

Yamashima T. 2000. Implication of cysteine proteases calpain, cathepsin and caspase in ischemic neuronal death of primates. Prog Neurobiol 62:273–295.

Yoshida M, Yamashima T, Zhao L, Tsuchiya K, Kohda Y, Tonchev AB, Matsuda M, Kominami E. 2002. Primate neurons show different vulnerability to transient ischemia and response to cathepsin inhibition. Acta Neuropathol (Berl) 104:267–272.

Zhang RL, Zhang ZG, Zhang L, Chopp M. 2001. Proliferation and differentiation of progenitor cells in the cortex and the subventricular zone in the adult rat after focal cerebral ischemia. Neuroscience 105: 33–41.

Zhang R, Zhang Z, Wang L, Wang Y, Gousev A, Zhang L, Ho KL, Morshead C, Chopp M. 2004. Activated neural stem cells contribute to stroke-induced neurogenesis and neuroblast migration toward the infarct boundary in adult rats. J Cereb Blood Flow Metab 24: 441–448.

Neuroscience xx (2006) xxx

TRANSCRIPTION FACTOR PROTEIN EXPRESSION PATTERNS BY NEURAL OR NEURONAL PROGENITOR CELLS OF ADULT MONKEY SUBVENTRICULAR ZONE

A. B. TONCHEV,[a,b] T. YAMASHIMA,[a]* K. SAWAMOTO[c,d] AND H. OKANO[d]

[a]*Department of Restorative Neurosurgery, Division of Neuroscience, Kanazawa University Graduate School of Medical Science, Takara-machi 13-1, Kanazawa 920-8641, Japan*

[b]*Division of Cell Biology, Department of Forensic Medicine, Varna University of Medicine, 55 Marin Drinov str, BG-9002 Varna, Bulgaria*

[c]*Bridgestone Laboratory of Developmental and Regenerative Neurobiology, Keio University School of Medicine, Tokyo, Japan*

[d]*Department of Physiology, Keio University School of Medicine, Tokyo, Japan*

Abstract—The anterior subventricular zone of the adult mammalian brain contains progenitor cells which are upregulated after cerebral ischemia. We have previously reported that while a part of the progenitors residing in adult monkey anterior subventricular zone travels to the olfactory bulb, many of these cells sustain location in the anterior subventricular zone for months after injury, exhibiting a phenotype of either neural or neuronal precursors. Here we show that ischemia increased the numbers of anterior subventricular zone progenitor cells expressing developmentally regulated transcription factors including Pax6 (paired-box 6), Emx2 (empty spiracles-homeobox 2), Sox 1–3 (sex determining region Y-box 1–3), Ngn1 (neurogenin 1), Dlx1,5 (distalless-homeobox 1,5), Olig1,3 (oligodendrocyte lineage gene 1,3) and Nkx2.2 (Nk-box 2.2), as compared with control brains. Analysis of transcription factor protein expression by sustained neural or neuronal precursors in anterior subventricular zone revealed that these two cell types were positive for characteristic sets of transcription factors. The proteins Pax6, Emx2, Sox2,3 and Olig1 were predominantly localized to dividing neural precursors while the factors Sox1, Ngn1, Dlx1,5, Olig2 and Nkx2.2 were mainly expressed by neuronal precursors. Further, differences between monkeys and non-primate mammals emerged, related to expression patterns of Pax6, Olig2 and Dlx2. Our results suggest that a complex network of developmental signals might be involved in the specification of primate progenitor cells. © 2006 Published by Elsevier Ltd on behalf of IBRO.

Key words: cerebral ischemia, primate, adult neurogenesis, cell fate, developmental signal.

*Corresponding author. Tel: +81-76-265-2381; fax: +81-76-234-4264.
E-mail address: yamashim@med.kanazawa-u.ac.jp (T. Yamashima).

Abbreviations: BrdU, 5-bromo-2′-deoxyuridine; CNP, 2′,3′-cyclic nucleotide 3′-phosphodiesterase; Dlx, distalless-homeobox; Emx, empty spiracles-homeobox; GFAP, glial fibrillary acidic protein; Ngn, neurogenin; Nkx, Nk-box; Olig, oligodendrocyte lineage gene; Pax, paired-box; Sox, sex determining region Y-box; SVZa, anterior subventricular zone; TRITC, tetramethylrhodamine isothiocyanate.

0306-4522/06$30.00+0.00 © 2006 Published by Elsevier Ltd on behalf of IBRO.
doi:10.1016/j.neuroscience.2006.01.053

The subventricular zone of the anterior horn of the lateral ventricle (SVZa) in the brain of adult mammals contains multipotent neural progenitor cells which are a subject of intensive research, predominantly using rodent models (reviewed by Gage, 2000; Okano 2002). Although studied less extensively in adult primates, SVZa precursor cells were documented also at the primate level, *in vitro* (Pincus et al., 1998; Roy et al., 2000) and *in vivo* (Kornack and Rakic, 2001; Pencea et al., 2001). Cerebral ischemia increases the proliferation of the precursor cells residing in SVZa, in both focal (Jin et al., 2001; Zhang et al., 2001; Arvidsson et al., 2002; Parent et al., 2002) and global (Iwai et al., 2003) rodent models. Recently, we confirmed the preservation of this phenomenon in primates by labeling precursor cells in adult macaque monkey brains with the thymidine analog 5-bromo-2′-deoxyuridine (BrdU). We found that the proliferation of monkey SVZa progenitors peaked early after ischemia, and that while most of these cells were destined for the olfactory bulb, some precursors retained an immature phenotype and location in SVZa for months after injury (Tonchev et al., 2005). A similar phenomenon of sustained progenitor existence in SVZa had been previously described in developing monkey brain (Ourednik et al., 2001), but the molecular signals involved in this precursor cell retention as well as in the overall regulation of primate SVZa progenitors remain unknown.

A central role in the regulation of neural development is played by families of region- and cell type-selective transcription factors that determine fundamental decisions regarding the behavior and fate of selective progenitor cell populations in the embryonic brain (reviewed by Monuki and Walsh, 2001; Shirasaki and Pfaff, 2002; Schuurmans and Guillemot, 2002). Expression of several of these developmental signals has been shown in adult rodent SVZa precursors, including paired-box (Pax) 6 (Heins et al., 2002; Hack et al., 2004), empty spiracles-homeobox (Emx) 2 (Galli et al., 2002), distalless-homeobox (Dlx) 2 (Doetsch et al., 2002), sex determining region Y-box (Sox) 2 (Ferri et al., 2004; Komitova and Eriksson, 2004), and oligodendrocyte lineage gene (Olig) 2 (Hack et al., 2004). At present, however, little is known of transcription factor expression by progenitor cells in adult primate SVZa.

In the present study, we investigated whether BrdU-positive ($BrdU^+$) progenitor cells in adult monkey SVZa express developmentally-regulated transcription factors, under normal conditions or after ischemia. We combined BrdU labeling at both short- and long-term intervals after ischemia with immunostaining for Ki67 to identify progenitors in active phases of cell cycle, or with markers of

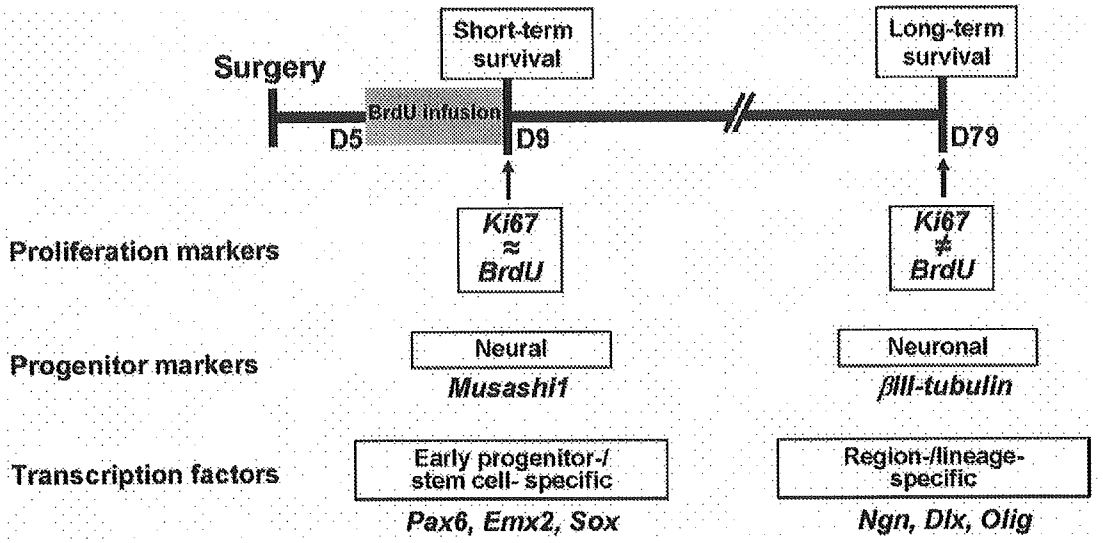

Fig. 1. Schematic presentation of BrdU/Ki67 paradigm and the investigation of transcription factor expression by progenitor cells in SVZa. BrdU infusion (gray bar) was performed between days 5–9 (D5–D9) after surgery, and the fate of $BrdU^+$ cells in SVZa was investigated on D9 (short-term interval) or at long-term intervals (D23, D44 and D79; D23 and D44 are omitted for clarity). As Ki67 selectively labels the proliferating cells at time of animal kill (arrows), at the D9 time-point almost all $BrdU^+$ cells are also $Ki67^+$, while at the long-term intervals after surgery only few $BrdU^+$ are co-labeled by Ki67. Cellular phenotypes characterized by their positivity for BrdU/Ki67 and Musashi1/βIII-tubulin (neural/neuronal) were investigated for putative expression of either early- or lineage-selective transcriptional regulators of embryonic brain development.

neural (Musashi1; Sakakibara et al., 1996; Sakakibara and Okano, 1997; Kaneko et al., 2000) or neuronal (βIII-tubulin; Pencea et al., 2001) progenitors to discern which is the cell type expressing a certain transcription factor (Fig. 1). Transcription factors targeted in our study were selected based on their expression by precursor cells in embryonic vertebrate telencephalon. We first explored markers of early multipotential stem/progenitor cells: Pax6 (Muzio et al., 2002), Emx2 (Heins et al., 2001), and Sox1–3 (Bylund et al., 2003). We then investigated transcription factors which are known to be specific for region- or lineage-restricted forebrain precursors: dorsal telencephalic markers such as neurogenin (Ngn) proteins (Schuurmans and Guillemot, 2002; Schuurmans et al., 2004), and ventral telencephalic markers such as Dlx (Anderson et al., 1997; Letinic et al., 2002; Stenman et al., 2003; Perera et al., 2004) and Olig (Schuurmans and Guillemot, 2002; Rowitch, 2004) proteins (Fig. 1). Our results suggest that some of these transcriptional regulators are expressed by adult primate SVZa progenitor cells and thus may be involved in their regulation.

EXPERIMENTAL PROCEDURES

Monkeys

Animal experiments were performed under the guidelines of the Animal Care and Ethics Committee of Kanazawa University, and the NIH Guide for the Care and Use of Laboratory Animals. Throughout the experiments, all efforts were made to minimize the number of animals used, and their suffering. Sexually mature female Japanese monkeys (*Macaca fuscata*) ($n=14$) were bred in air-conditioned cages, and were allowed free daily access to food and water. Transient global cerebral ischemia was performed under general inhalation anesthesia with artificial ventilation as previously described (Yamashima, 2000; Yamashima et al., 1998; Tonchev et al., 2005). Briefly, after resecting the sternum, the innominate and left subclavian arteries were transiently clipped for 20 min. The effectiveness of clipping was demonstrated by an almost complete absence (0.5±1.0 ml/100 g brain/min) of cerebral blood flow being monitored by laser Doppler (Vasamedics, St. Paul, MN, USA). Ischemia was performed to eight macaques, while six macaques underwent sham surgery (executed by opening the chest without vessel clipping). All monkeys received five daily injections of 100 mg/kg i.v. of BrdU (Sigma-Aldrich Japan K.K., Tokyo, Japan), performed on days 5–9 after surgery. Respective animals were then killed on day 9 ($n=2$), day 23 ($n=2$), day 44 ($n=2$) and day 79 ($n=2$) after ischemia or on day 9 ($n=2$), day 23 ($n=2$) and day 44 ($n=2$) after the sham operation (Tonchev et al., 2005).

Tissue processing

The monkeys were killed by intracardial perfusion with 4% paraformaldehyde under general anesthesia. The brains were removed, and tissue blocks (ac +7 mm anteriorly to ac +1 mm posteriorly) were cryoprotected in sucrose, and frozen in O.C.T. medium (Tissue-Tek, Sakura Finetech Co, Tokyo, Japan), and serially cut into 40-μm thick coronal sections. All stainings were performed on free-floating sections. To reveal BrdU incorporated into the cells, DNA was denatured by treatment with formamide and HCl as described (Eriksson et al., 1998; Tonchev et al., 2003), followed by application of mouse anti-BrdU (1:100, Becton Dickinson, San Jose, CA, USA) or rat anti-BrdU (1:100, Harlan Sera-Laboratory, Loughborough, UK) antibodies. We used the following antibodies for phenotypic markers: mouse anti-Ki67 (1:50, Novocastra, Newcastle, UK), rat anti-Musashi1 (1:100, Kaneko et al., 2000), rabbit anti-Musashi1 (1:200, Chemicon, Temecula, CA, USA), rabbit or mouse anti-Nestin (1:200, Chemicon), mouse anti-NeuN (1:100, Chemicon), rabbit or mouse anti-β-tubulin class III (1:400, Covance, Richmond, CA, USA), goat anti-Doublecortin (1:200; Santa Cruz Inc., Santa Cruz, CA, USA), mouse anti-2′,3′-cyclic nucleotide 3′-phosphodiesterase (CNP) (1:400; Chemicon),

and rabbit anti-glial fibrillary acidic protein (GFAP) (1:400, Sigma). The following rabbit polyclonal antibodies against transcription factors were obtained from Chemicon: Emx2 (1:400), Ngn1 (1:2000), Ngn2 (1:1500), Ngn3 (1:100–1:1000), Dlx1 (1:500), Dlx2 (1:200), Dlx5 (1:1000), Sox1 (1:200), Sox2 (1:200), Sox3 (1:200), Olig1 (1:1000), Olig3 (1:300), Nkx2.2 (1:400). The rabbit Pax6 antibody (1:200) was from Covance, and the rabbit anti-Olig2 antibody was a gift from Hirohide Takebayashi (National Institute for Physiological Sciences, Okazaki, Japan).

The primary antibodies were revealed by appropriate secondary antibodies conjugated to AlexaFluor 488, 546, or 633 (Molecular Probes, Eugene, OR, USA), tetramethylrhodamine isothiocyanate (TRITC; Jackson Immunoresearch, West Grove, PA, USA), or to biotin for immunoperoxidase labeling (1:30–1:100; Vector ABC kit, Vector Laboratories, Burlingame, CA, USA). For double- and triple-staining, the respective primary antibodies were from different species, and were applied sequentially to minimize the probability for cross-reactivity. Negative control experiments were performed by omitting the primary antibody and these revealed no positive staining.

Image analysis

Double- and triple-labeling to determine the expression of transcription factors by BrdU-labeled cells or cells labeled for particular phenotypic markers was evaluated using confocal laser scanning microscopy (LSM 510, Carl Zeiss, Tokyo, Japan). Alexa Fluor 488 was appointed in the green channel, TRITC or Alexa Fluor 546, in the red channel, and Alexa Flour 633, in the blue channel. Each fluorochrome was scanned separately and sequentially to minimize the probability of signal transfer among channels. Z sectioning at 0.5–1 μm intervals was performed and optical stacks of at least 20 images were used for analysis. Digital three-dimensional reconstructions were created by the Zeiss LSM software version 2.3. Within each animal group, at least 150 cells positive for BrdU or a phenotypic marker were sampled for co-expression with respective transcription factors. The absolute numbers of transcription factor/BrdU double-positive cells were determined by multiplying the corresponding fractions with the total numbers of $BrdU^+$ cells evaluated on every 12th section stained by the peroxidase method within grids of 800 μm×100 μm placed in the dorsal, ventral, and striatal aspects of SVZa (see Fig. 2A) as previously described (Tonchev et al., 2005). Numbers and percentages were averaged to obtain a mean density value for each transcription factor/animal group.

Statistical analysis

For comparing percentages of cells expressing certain transcription factor, we applied nonparametric tests (Mann-Whitney *U* test and Kruskal-Wallis test) or one-way ANOVA followed by Tukey-Kramer's post hoc comparisons. Data were expressed as means±S.E.M. Differences were considered significant when $P<0.05$.

RESULTS

Expression of Pax6, Emx2 and Sox proteins by SVZa progenitors

Immunohistochemical staining for the transcription factors Pax6, Emx2, and Sox1–3 revealed numerous positive cells, frequently in clusters, located along the walls of the anterior horn of the lateral ventricle (Fig. 2A, arrows), the zone that contains proliferating ($BrdU^+$) precursor cells in the adult mammalian brain (Fig. 2A, arrowheads). At the early post-BrdU time-point (day 9 after surgery, 2 h after the last BrdU injection), most (75–85%) $BrdU^+$ cells in SVZa co-expressed Pax6 (Fig. 2B, 2F1), Emx2 (Fig. 2C, 2F2) and Sox2,3 (Fig. 2F4, F5). The $Sox1^+/BrdU^+$ cells composed about half of the $BrdU^+$ cells (Fig. 2D, 2F3). At a late post-BrdU survival time-point (day 44 after surgery, 5 weeks after the last BrdU injection), many of the $BrdU^+$ cells that had retained their presence in SVZa revealed negativity for the transcription factors (Fig. 2E, arrows). The percentage of $BrdU^+$ cells expressing Pax6, Emx2 or Sox2,3 decreased with a statistical significance ($P<0.05$, Kruskal-Wallis test), while the Sox1/BrdU co-labeling sustained its value (Fig. 2F). While no statistically significant difference was found between sham-operated and ischemic brains with respect to the percentage of $BrdU^+$ cells expressing the five transcription factors (Fig. 2F), the absolute numbers of BrdU/transcription factor double-positive cells in postischemic SVZa was significantly greater than in the controls (Fig. 2G).

To investigate the progenitor cell type(s) expressing Pax6, Emx2 and Sox1–3, we performed co-labeling with Musashi1, a marker of neural progenitor cells (Kaneko et al., 2000), and with βIII-tubulin or Doublecortin, markers of progenitors committed to neuronal lineage (neuronal progenitors) (Pencea et al., 2001; Gleeson et al., 1999). We observed that Pax6 (Fig. 3A, 3H1), Emx2 (Fig. 3B, 3H2) and Sox2,3 (Fig. 3C, 3H3) co-stained exclusively with Musashi1 in both ischemic and sham-operated animals. Co-labeling with neuronal progenitor markers (Fig. 3D) was negligible for these four transcription factors (<1% of the $Pax6^+$, $Sox2,3^+$ cells, and<5% of the $Emx2^+$ cells). In contrast, Sox1 co-labeled mostly with βIII-tubulin (Fig. 3F, 3H4), while less than 3% of the $Sox1^+$ cells co-expressed Musashi1 (Fig. 3E, 3H4). The transcription factor-positive clusters remained negative for GFAP (Fig. 3G).

Differential transcription factor expression by sustained proliferating progenitors

We have previously documented the existence of long-term BrdU-retaining cells in SVZa that have incorporated BrdU early after ischemia and preserved an immature phenotype and location in SVZa for months after injury (Tonchev et al., 2005; see Fig. 1). Most of these $BrdU^+$ cells expressed βIII-tubulin indicating neuronal differentiation, while a few were positive for Musashi1 and Ki67 suggesting they were neural progenitors in active phases of their cell cycle (Tonchev et al., 2005). We investigated whether BrdU/Ki67 double-positive cells co-express transcription factors at long-term time-points after ischemia/BrdU. Triple-labeling for BrdU, Ki67 and the five transcription factors on postischemic days 44 or 79 (5 or 10 weeks after BrdU, respectively) revealed that the vast majority of the $BrdU^+/Ki67^+$ cells in SVZa were co-labeled for Emx2 (Fig. 4A; 47 of 53 $BrdU^+/Ki67^+$ cells), Pax6 (Fig. 4B; 43 of 51), Sox2 (Fig. 4C; 50 of 55) or Sox3 (51 of 57). In contrast, Sox1 expression was not found in $BrdU^+/Ki67^+$ cells (Fig. 4D). Additional experiments provided direct evidence that the $Ki67^+$ cells were $Musashi1^+$ (Fig. 4E, arrowheads) but negative for βIII-tubulin (Fig. 4E, arrows), and that Musashi1 was expressed by sustained $BrdU^+/Sox3^+$ cells (Fig. 4F), and similarly, by sustained $BrdU^+/$

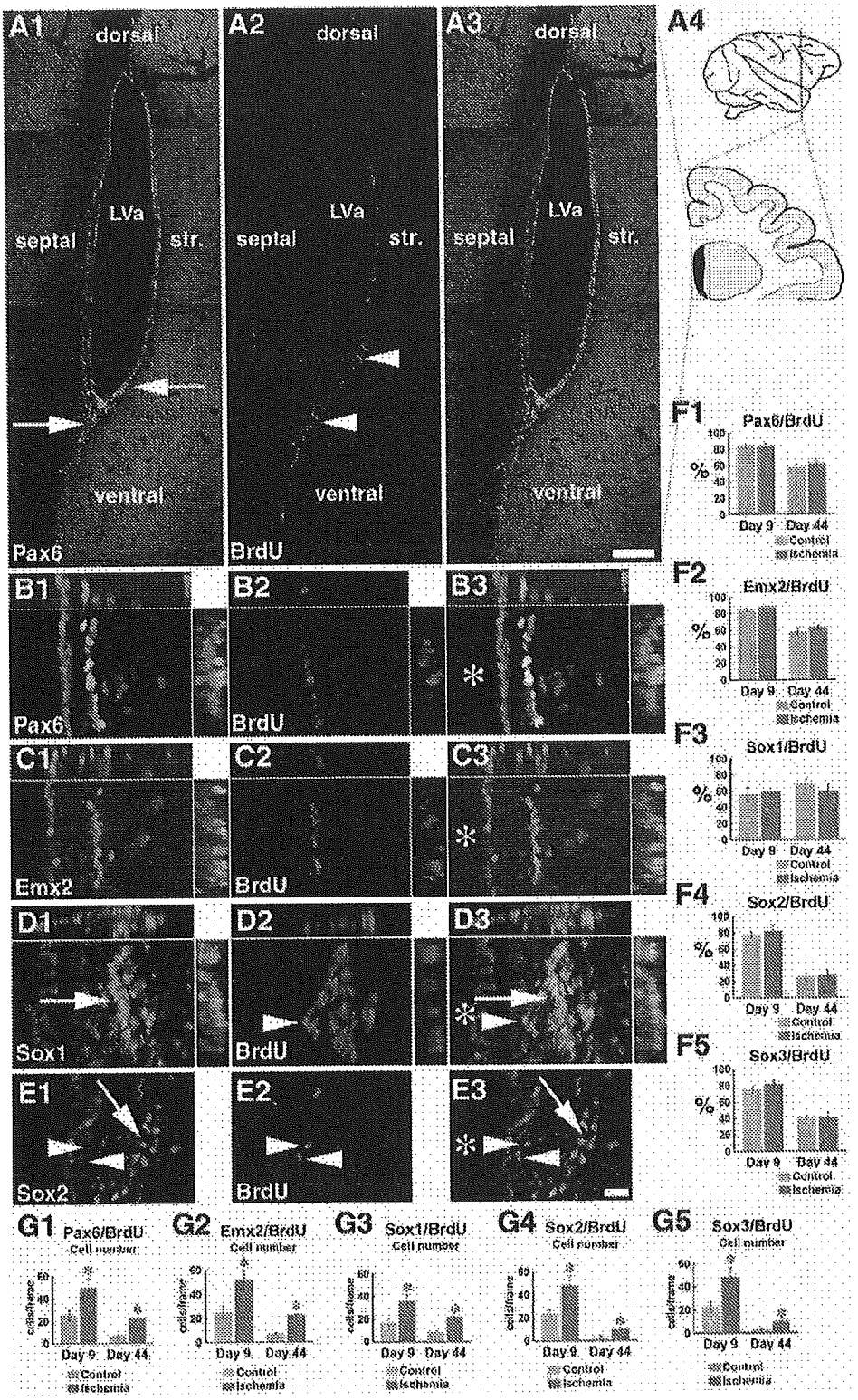

Fig. 2. Expression of Pax6, Emx2 and Sox proteins by BrdU$^+$ cells in monkey SVZa. (A) Low magnification micrographs showing the overall distribution of Pax6 (A1) and BrdU (A2) positive signals in SVZa, and overlay (A3). The position of the anterior horn of the lateral ventricle (LVa) sampled in A1–A3 is depicted on the schematic map (A4). Note that both Pax6$^+$ cells (arrows) and BrdU$^+$ cells (arrowheads) are preferentially located along the walls of LVa, not in the parenchyma. The images are representative also for the other four transcription factors. Str., striatal SVZa. (B) High

$Sox2^+$, $BrdU^+/Pax6^+$ and $BrdU^+/Emx2^+$ cells (data not shown).

Expression of Ngn proteins by SVZa progenitors

Double-labeling for BrdU and Ngn1 (Fig. 5A) or Ngn2 (Fig. 5B) revealed contrasting findings. The $Ngn1^+/BrdU^+$ cells comprised a significant proportion of the $BrdU^+$ cells (60–70% on day 9; 35–40% on day 44), while the $Ngn2^+/BrdU^+$ cells were few (less than 5% of the $BrdU^+$ cells on day 44) (Fig. 5C1, 5C2). The $Ngn1^+/BrdU^+$ cells were typically grouped within a larger $Ngn1^+$ cluster (Fig. 5A, box). The rare $Ngn2^+/BrdU^+$ cells were entangled in the $BrdU^+$ clusters (Fig. 5B4–5B6, arrows) as were some $Ngn2^+/BrdU^-$ cells (Fig. 5B4–5B6, arrowheads). No statistically significant difference was found between sham-operated and ischemic brains with respect to the percentage of $BrdU^+/Ngn^+$ cells, while the absolute numbers of $BrdU^+/Ngn1^+$ (but not $BrdU^+/Ngn2^+$) cells in postischemic SVZa were significantly greater than in the controls (Fig. 5C3, 5C4). A third member of the family, Ngn3, was not found to be expressed in SVZa in our experiments (data not shown).

Co-staining with progenitor cell markers also revealed differences between Ngn1 and Ngn2. Ngn1 and Musashi1 co-labeled extensively (Fig. 5D) forming large (more than 10 cells) double-labeled clusters, with the $Ngn1^+/Musashi1^+$ cells comprising 70–75% of the $Ngn1^+$ cells on day 9 (Fig. 5H1). In contrast, only a third of the $Ngn2^+$ cells co-stained with Musashi1 (Fig. 5E, 5H1). $Ngn1^+$ clusters smaller than the $Ngn1^+/Mushashi1^+$ clusters (typically up to five cells) expressed βIII-tubulin (Fig. 5F, arrows), and Ngn1/βIII-tubulin co-labeling increased at long-term time points (Fig. 5J1). In addition, $Ngn1^+$ clusters were closely associated with $\beta III\text{-tubulin}^+$ aggregates (Fig. 5F, arrowheads), although most of the $Ngn1^+$ cells themselves were negative for βIII-tubulin. Only single rare $Ngn2^+$ cells co-labeled with βIII-tubulin (Fig. 5G, arrows). $Ngn1^+$ cells expressed Ki67 on day 9 (Fig. 5H), but not at long-term time points (Fig. 5I).

Expression of Dlx proteins by SVZa progenitors

Double-labeling experiments with BrdU and antibodies against Dlx1,2,5 revealed that clusters positive for Dlx1 (Fig. 6A) and Dlx5 (Fig. 6C) extensively co-labeled with BrdU. In contrast, Dlx2/BrdU co-staining (Fig. 6B) was minimal (<2% of the $BrdU^+$ cells). The percentage of $BrdU^+$ cells double-stained for Dlx1 or Dlx5 was 70–75% on day 9 decreasing (with a statistical significance, $P<0.01$, Kruskal-Wallis test) to 35–40% on day 44 (Fig. 6D1, 6D2). No statistically significant difference was found between sham-operated and ischemic brains ($P>0.05$, Kruskal-Wallis test). The absolute numbers of $BrdU^+/Dlx1^+$ (Fig. 6D3) and $BrdU^+/Dlx5^+$ (Fig. 6D4) cells in postischemic SVZa were significantly greater than in the controls.

Double-labeling for Dlx1,5 and Musashi1 revealed that both $Dlx^+/Musashi1^+$ cells (Fig. 6E, arrows) and $Dlx^-/Musashi1^+$ cells (Fig. 6E, arrowheads) were aggregated in a common cluster. Dlx1 did not co-label with Ki67 at long-term survival time-points (Fig. 6F), and neither did Dlx2 nor Dlx5 (data not shown). The $Dlx1^+/Musashi1^+$ and $Dlx5^+/Musashi1^+$ cells were numerous (Fig. 6I), while only rare $Dlx2^+/Musashi1^+$ cells were observed (data not shown). Both Dlx1 and Dlx5 co-stained with βIII-tubulin (Fig. 5G, 5I), and notably, with sustained neuronal progenitors ($BrdU^+/\beta III\text{-tubulin}^+$ cells) at long-term survival time-points after BrdU (Fig. 5H). Dlx2 did not co-label with βIII-tubulin or Doublecortin (data not shown).

Expression of Olig proteins by SVZa progenitors

Double-staining for BrdU and Olig1 or Olig3 demonstrated that the two transcription factors extensively co-labeled with BrdU on day 9 (Fig. 7A), while at long-term survival (day 44) the percentage of co-staining with BrdU significantly decreased (Fig. 7B, 7E1, 7E2). In contrast, $Olig2^+$ clusters (Fig. 7C, arrows) did not co-label with BrdU (Fig. 7C, arrowheads), and only single weakly labeled $Olig2^+$ cells rarely co-stained with BrdU (<1% of the $BrdU^+$ cells). We also investigated Nkx2.2, a factor that is also involved in the control of oligodendrogenesis in both embryonic and adult brain (Rowitch, 2004; Fancy et al., 2004). Similarly to Olig1,3, Nkx2.2 (Fig. 7D) extensively co-labeled with BrdU at short-term survival time-points, while at long-term survival (day 44) the percentage of co-staining with BrdU decreased (Fig. 7E3) with a statistical significance ($P<0.05$, Kruskal-Wallis test). The percentage of Nkx2.2/BrdU co-labeling (45–50%) was significantly higher than the percentage of Olig1/BrdU or Olig3/BrdU co-labeling (10–15%) ($P<0.01$, Kruskal-Wallis test). The absolute numbers of $BrdU^+/Olig1^+$ (Fig. 7E4), $BrdU^+/Olig3^+$ (Fig. 7E7) and $BrdU^+/Nkx2.2^+$ (Fig. 7E6) cells in postischemic SVZa were significantly greater than in the controls.

Dual immunohistochemical staining with Musashi1 resulted in co-labeling with Nkx2.2, Olig1 and Olig3 (Fig. 7F, 7J), but not with Olig2 (data not shown). On the other hand, Olig3 and Nkx2.2 (but not Olig1 or Olig2) co-stained with βIII-tubulin in SVZa (Fig. 7G, 7J), while Nkx2.2 and Olig2 co-labeled with the oligodendrocyte marker CNP (Braun et al., 1988) in the adjacent striatal parenchyma (Fig. 7H). At long-term survival time-points after BrdU Olig1 (but not

power view of Pax6 (B1) and BrdU (B2) double-staining on day 9, and overlay of the channels (B3). (C) Staining for Emx2 (C1) and BrdU (C2) on day 9, and overlay (C3). (D) Staining for Sox1 (D1) and BrdU (D2), and overlay (D3), day 44. Note that while most cells within the cluster are double-positive (arrows), a few are $Sox1^-/BrdU^+$ (arrowheads). Staining of Sox1 is representative also for Sox2,3 on day 9. Orthogonal projections in the *x* and *y* axes (right and top of each image in B–D) confirm co-labeling. (E) Sox2/BrdU double-staining on day 44 (long-term survival after surgery/BrdU). Many of the $BrdU^+$ cells (arrowheads) are not co-labeled by Sox2 (arrows). Image is representative also for Sox3. (F) Percentage of $BrdU^+$ cells co-labeled for Pax6 (F1), Emx2 (F2), Sox1 (F3), Sox2 (F4) or Sox3 (F5), at short-term (day 9) or long-term (day 44) survival after surgery/BrdU. (G) Absolute number of $BrdU^+$ cells co-labeled for Pax6 (G1), Emx2 (G2), Sox1 (G3), Sox2 (G4) or Sox3 (G5). * $P<0.05$ versus control. Scale bar=200 μm (A); 20 μm (B–E). Asterisk, lateral ventricle.

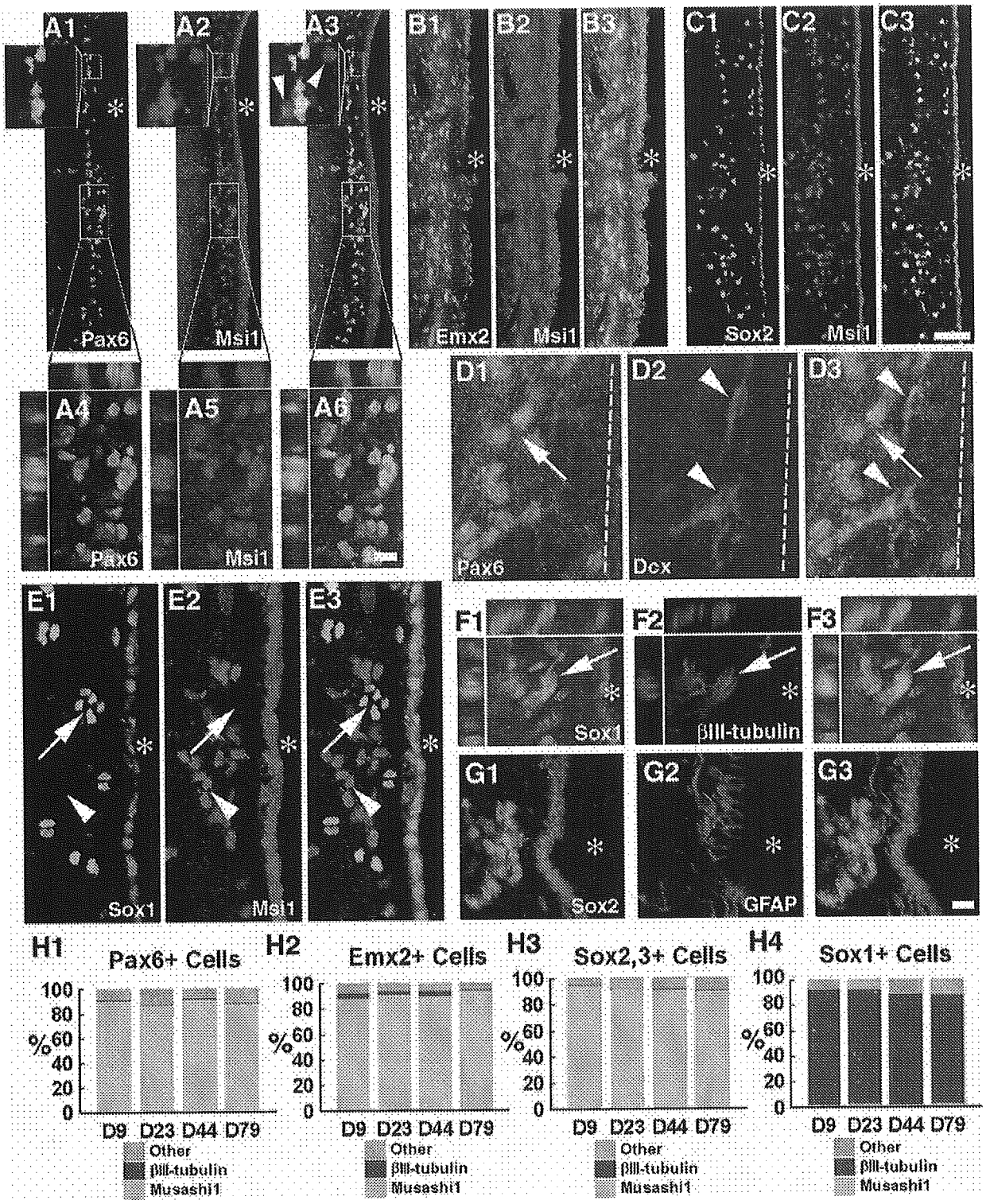

Fig. 3. Co-labeling of Pax6, Emx2 and Sox proteins with progenitor cell markers. (A) Double-staining for Pax6 (A1) and Musashi1 (Msi1, A2), and overlay (A3), on day 9. Two regions (depicted in frames) in the low magnification micrograph are shown in magnification in the insets. The upper inset demonstrates that despite extensive co-labeling, single-labeled cells were also observed (arrowheads). The lower inset (A4–A6) shows confirmation of double-staining by computer-generated orthogonal projections. (B) Double-staining for Emx2 (B1) and Musashi1 (B2), and overlay (B3), on day 9. (C) Double-staining for Sox2 (C1) and Musashi1 (C2), and overlay (C3), on day 44. (D) Double-staining for Pax6 (D1; a positive "doublet" is depicted